Agriculture, Trade and Biodiversity*

Chloé Antoine†

March 2026

[PRELIMINARY AND INCOMPLETE]

Abstract

Does agricultural trade liberalization erode biodiversity, or can it help preserve it? This paper develops the first quantitative trade model in which biodiversity is an endogenous outcome. Building on a Ricardian multi-country general equilibrium framework with explicit extensive and intensive margins of land use, I embed two ecological sub-modules that translate simulated land-use patterns into long-run species richness and dynamic population abundance. I focus the empirical analysis on birds, which are widely regarded as the premier indicators of overall ecosystem health. I find that the liberalization that took place between 1980 and 2011 has, on average, helped reduce bird species loss globally, primarily by curbing the expansion of low-intensity farming. This aggregate benefit, however, conceals a steep distributional cost: liberalization shifts production toward biodiversy-rich regions, raising extinction risk in some southern ecoregions by up to 34.5%, while northern ecoregions benefit. Trade-induced land-use changes also leave a modest but persistent imprint on bird population dynamics. I further trace the feedback from trade-induced biodiversity change to agricultural productivity and, subsequently, food security and welfare.

Keywords: agriculture, trade policy, biodiversity, land-use, birds
JEL Codes: F18, Q15, Q17, Q57

*For fruitful discussions and valuable comments, I am particularly grateful to Greoffrey Barrows, Jean-Marc Bourgeon, Gregory Corcos, Christophe Gouel, Ishan Nath, Frederik Noack, Anna Russo and Wolfram Schlenker. I also thank the seminar participants at CREST, AMSE, CEE-M, CESCO, Harvard and Duke, as well as the attendees of the E4C Summer School and ETSG Conference, for their insightful questions and constructive feedback. Annette Delatour provided excellent research assistance on bird data. Part of this project was carried out during my visit to the Mossavar-Rahmani Center for Business and Government at the Harvard Kennedy School during the spring term of 2026. In this regard, I gratefully acknowledge financial support from the Fulbright Visiting Student Researcher Program and the EUR 'DATA EFM' at CREST, as well as material support from the Salata Institute for Climate and Sustainability at Harvard University. All errors are my own.

†Centre for Research in Economics and Statistics (CREST), École Polytechnique, Institut Polytechnique de Paris. Email: chloe.antoine@ensae.fr.

1 Introduction

The world has lost roughly one-third of its wild vertebrate populations since 1970, and agriculture is the single largest driver of that collapse (WWF, 2024). Over the same period, the conditions under which agricultural goods are traded have been transformed. Protection rates in high-income countries peaked around the mid-1980s and have declined markedly since, through successive GATT and WTO rounds as well as a wave of regional trade agreements that have progressively reduced tariffs and non-tariff barriers on food and agricultural products (Anderson et al., 2008). Containerization meanwhile halved maritime freight costs (Hummels, 2007), and the global market for agricultural inputs—seeds, fertilizers, pesticides, and machinery—became deeply integrated. Whether these two trends are causally linked, and in which direction, is unknown. This paper asks a question whose answer has profound consequences for both environmental policy and the design of trade agreements: does freer agricultural trade erode biodiversity, or can it help preserve it?

The stakes of this question extend beyond species counts. Because wildlife underpins the pest control, pollination, and nutrient cycling on which agricultural yields depend (Mariyappan et al., 2023), biodiversity loss feeds back into food production, trade, and welfare. If trade liberalization accelerates biodiversity loss, then the gains from comparative advantage come at an unaccounted ecological price that ultimately rebounds on agriculture itself. If instead it encourages land-sparing by concentrating production where it is most efficient, free trade may be a powerful tool for conservation.

The difficulty in answering this question is that trade liberalization operates through two channels that pull in opposite directions. On the extensive margin, allowing countries to specialize according to comparative advantage reduces the total land area needed to feed the world, potentially sparing natural habitats from conversion. On the intensive margin, cheaper access to fertilizers, pesticides, and machinery lowers the cost of high-input farming, intensifying the ecological footprint of every hectare in production. This intensive-margin effect is not benign: pesticides directly harm wildlife through lethal exposure and sublethal effects on reproduction and migration (Lopez-Antia et al., 2015; Eng, Stutchbury, and Morrissey, 2019), while fertilizer runoff degrades the aquatic and terrestrial habitats on which many species depend (Rigal et al., 2023). The net effect on biodiversity is therefore theoretically ambiguous, empirically unquantified, and almost certainly heterogeneous across space—what spares a forest in Europe may accelerate conversion in the Amazon.

I build a framework capable of resolving this ambiguity. I introduce a Ricardian multi-country general equilibrium trade model in which land-use and biodiversity are jointly determined endogenous outcomes. Building on Farrokhi and Pellegrina (2023), the production side features a fixed cost of converting natural habitat to agricultural use, generating an endogenous agricultural frontier, and distinguishes two crop-production technologies—traditional (low-input) and modern (high-input). Farmers draw land productivities from nested Fréchet

distributions, choosing simultaneously which crop to grow and which technology to adopt. This structure generates responses to trade-cost changes at both the extensive and intensive margins. Goods are traded across countries through a hub-and-spoke system subject to iceberg costs, with domestic trade costs linking individual fields to national hubs. Consumers aggregate varieties across origins through a three-tier Armington structure. The framework also incorporates a livestock sector following Gouel and Laborde (2021), in which livestock producers combine labor with a CES feed-mix of tradable crops and domestically produced grass, essential for capturing the 68% of global agricultural land used for grazing that prior models have largely ignored.

Biodiversity enters the model through two ecological sub-modules that translate simulated land-use patterns into ecological outcomes, which constitutes the core methodological innovation of this paper. The first sub-module applies a Countryside Species-Area relationship (Pereira and Daily, 2006; Chaudhary et al., 2015; Scherer et al., 2023) to map the spatial distribution of land-use types—traditional agriculture, modern agriculture, pasture, and natural habitat—onto long-run species richness, measured as the number of species committed to extinction in each ecoregion. The second tracks population dynamics through a discrete-time Verhulst growth equation, in which the maximum population size each habitat can sustainably support depends on cropland area, pasture, pesticide use, and seasonal climate (Mouysset et al., 2019; Cocco, Kervinio, and Mouysset, 2023). Both sub-modules can be applied to any taxon, making the framework broadly applicable.

I focus the empirical analysis on birds. Birds are the most extensively monitored taxonomic group on the planet and occupy multiple trophic levels, making them uniquely sensitive to environmental disturbances at every level of the food chain. This sensitivity means that patterns observed in avian communities are highly informative about the health of ecosystems more broadly, which is why birds are widely regarded as the premier indicator of overall ecological integrity (Padoa-Schioppa et al., 2006). They are also the group for which the feedback loop to agriculture is best documented: birds provide pest control, pollination, and seed dispersal services whose loss has been shown to measurably reduce agricultural productivity (Noack, Engist, and Larsen, 2025), making them a first-order concern for any model that seeks to close the loop between economic and biodiversity outcomes.

The trade-land-use core is calibrated for 66 countries and 822,053 five-arc-minute fields, covering 36 tradable agricultural outputs and three agricultural inputs. Production and bilateral trade flows are drawn from BACI-CEPII, FAOSTAT, and GTAP, while production-technology parameters are derived from the Global Agro-Ecological Zones (GAEZ) potential-yield database. Demand elasticities and bilateral trade cost parameters are estimated from gravity equations, using GAEZ potential yields as instruments for agricultural prices. The species-richness module draws on characterization factors from Scherer et al. (2023) and is applied across all 698 world ecoregions. The abundance module focuses on the United States, where uniquely fine-resolution data are available: carrying-capacity parameters are estimated

for the 100 most abundant U.S. bird species across 393 Level-IV ecoregions using 25 years of count data from the North American Breeding Bird Survey, land-use and climate variables from ESA, and pesticide application data from the U.S. Geological Survey. The estimated model reproduces untargeted moments of cross-country agricultural input intensity and generates acreage elasticities consistent with the micro-level literature, providing confidence in the counterfactual predictions.

Under the observed 2011 trade regime, the baseline scenario predicts an average loss of 4.33 bird species per ecoregion, of which 3.15 are attributable to modern input-intensive farming and 1.17 to traditional low-intensity agriculture. Although agricultural land covers only 7% of the global land surface, roughly 72% of it is classified as modern, reflecting the degree to which high-input farming already dominates global agriculture. I run counterfactual exercises that reset trade costs in agricultural inputs and/or outputs to their 1980 levels—effectively simulating a world without the liberalization hat occurred between 1980 and 2011—and trace the consequences through both the economic and ecological components of the model.

Counterfactual simulations show that trade liberalization between 1980 and 2011 operated through two opposing channels: it reduced the total land area devoted to agriculture by over 10% but also increased the share of input-intensive farming within agricultural land by nearly 4%, exposing wildlife to higher levels of agrochemicals. On net, the land-sparing effect appears to dominate: reverting to 1980 trade costs would raise average species loss per ecoregion by 9%. This aggregate benefit, however, conceals a steep distributional cost. The spatial pattern of winners and losers runs along a stark north-south axis: northern ecoregions benefit most from liberalization, and would see extinction risk rise by up to 78% if trade costs reverted to 1980 levels. Southern biodiversity hotspots—those with the highest pre-Anthropocene species richness—experience the reverse effect: lower output trade costs shift crop production toward tropical and subtropical regions where agro-ecological conditions confer strong comparative advantage for many crops, concentrating habitat conversion where the marginal biodiversity cost per hectare—measured in species lost—is highest. Trade-induced land-use changes also leave a modest but persistent imprint on U.S. bird abundance. Simulated national-average abundances for three representative species shift by 0.3–1.2 percentage points over five years following the trade-cost shock, with the sign and magnitude varying across species according to their sensitivity to habitat change and pesticide exposure. The gap between baseline and counterfactual also widens over time, suggesting that the ecological consequences of today's trade policies may remain latent before compounding through population dynamics and potential tipping points. Eventually, I further trace the feedback from these biodiversity changes to agricultural productivity and welfare, closing a loop between economic and ecological outcomes.

Related literature. This paper sits at the intersection of three strands of the literature. The first is the literature on the biodiversity impacts of trade. Most existing work in this area

use input-output tables to attribute embodied species loss to bilateral trade flows (Chaudhary and Kastner, 2016; Cabernard, Pfister, and Hellweg, 2024). This approach quantifies where biodiversity loss is consumed, but cannot answer the counterfactual question of how biodiversity would differ under alternative trade policies. The closest antecedent to my structural approach is Polasky, Costello, and McAusland (2004), which derives theoretical conditions under which trade raises or lowers biodiversity in a two-country, two-good model with a species-area relationship. I extend that framework in four directions: a many-country, many-sector general equilibrium setting with incomplete specialization; an empirical implementation brought to data; an explicit intensive margin of land use; and a dynamic abundance metric alongside the static richness measure. The result is the first framework capable of identifying the extent to which trade *causes* biodiversity change.

The second strand is the growing literature on agriculture and the environment in quantitative trade models. Existing papers have examined climate change (Costinot, Donaldson, and Smith, 2014; Gouel and Laborde, 2021), deforestation (Dominguez-Iino, 2025; Farrokhi et al., 2025), and water resources (Carleton, Crews, and Nath, 2025). Biodiversity has been absent from this agenda, despite being an environmental outcome directly and mechanically tied to agricultural land use. This paper fills this gap. I build directly on the trade and land-use framework of Farrokhi and Pellegrina (2023), but depart from it in two substantive ways. First, I augment the model with two explicit biodiversity sub-modules, shifting the object of analysis from land-use reallocation as an economic outcome to land-use reallocation as the mechanism through which trade reshapes ecosystems. Second, I enrich the production side with a livestock sector and an expanded set of 36 tradable crops, improving the representation of comparative advantage and the realism of the mapping from trade policy to habitat conversion.

The third strand is the emerging economics of biodiversity and ecosystem services. A recent wave of papers has begun to quantify what biodiversity loss costs the economy. Frank and Sudarshan (2024) showed that the functional extinction of Indian vultures raised human mortality by more than 4% and generated roughly $70 billion in annual social costs. Noack, Engist, and Larsen (2025) estimated that the 30% decline in North American bird abundance has reduced U.S. agricultural sales by about 4% through diminished pest control and pollination. These papers establish the economic stakes of biodiversity loss. This paper investigates one potentially important driver—trade policy—and extends the analysis of consequences beyond agricultural productivity to include effects on land-use decisions and international trade flows. In doing so it closes a feedback loop that captures how changes in biodiversity *shape* and *are shaped* by economic outcomes.

The rest of the paper is organized as follows. Section 2 presents the model. Section 3 details the estimation strategy. Section 4 presents the counterfactual results, and Section 5 concludes.

2 Theory

In this section, I present the general equilibrium model that allows me to link changes in trade costs to changes in bird biodiversity. The model draws upon the works of Farrokhi and Pellegrina (2023) and Gouel and Laborde (2021) for the trade and land-use component, and of Scherer et al. (2023) and Cocco, Kervinio, and Mouysset (2023) for the biodiversity components.

2.1 Environment

I consider a world composed of multiple countries, indexed by $i \in \mathcal{I} \equiv \{1, \ldots, I\}$, and multiple ecoregions, indexed by $e \in \mathcal{E} \equiv \{1, \ldots, E\}$, which delimit distinct ecosystems. A country may contain several ecoregions, and an ecoregion may span several countries. Each country i is endowed with a quantity L_i of land, N_i of labor and V_i of raw fertilizer. Land is divided into heterogeneous fields f. Each field is located at the intersection of some country i, such that $\sum_{f \in \mathcal{F}_i} L_f = L_i$, and some ecoregion e, such that $\sum_{f \in \mathcal{F}_e} L_f = L_e$. All fields correspond to 5-arcminute grid cells and consist of a continuum of heterogeneous plots $\omega \in f$.

Goods are indexed by $g \in \mathcal{G}$ and include: (1) an outside good $g = 0$, (2) agricultural inputs, indexed by $j \in \mathcal{J} \subset \mathcal{G}$, and (3) agricultural outputs, indexed by $k \in \mathcal{K} \subset \mathcal{G}$. I consider that the bundle of agricultural outputs includes a livestock product, indexed by $k = \ell$, and a forage crop (grass), which is only used to feed livestock and cannot be internationally traded. The set of agricultural outputs can therefore be divided into two categories: tradable outputs, indexed by $k \in \mathcal{K}^a$, which include all crops except grass; and crops, indexed by $k \in \mathcal{K}^c$, which include all agricultural outputs except the livestock product.

2.1.1 Preferences

I assume that consumers' preferences follow a three-tier Armington structure. In the upper-tier, the representative household in field f derives utility from consuming the outside good composite, C^0_{fi}, and an agricultural composite, C^a_{fi} according to a CES aggregator:

$$C_{fi} = \left[\left(\beta_i^0\right)^{1/\eta} \left(C^0_{fi}\right)^{(\eta-1)/\eta} + \left(\beta_i^1\right)^{1/\eta} \left(C^a_{fi}\right)^{(\eta-1)/\eta} \right]^{\eta/(\eta-1)}, \tag{1}$$

where η is the elasticity of subsitution, β_i^0 and β_i^1 are exogenous demand shifters. In the middle-tier, the agricultural consumption bundle aggregates the consumption of tradable agricultural outputs $k \in \mathcal{K}^a$ according to CES preferences with elasticity of substitution κ and exogenous demand shifters b_i^k:

$$C^a_{fi} = \left[\sum_{k \in \mathcal{K}^a} \left(\beta_i^k\right)^{1/\kappa} \left(C^k_{fi}\right)^{(\kappa-1)/\kappa} \right]^{\kappa/(\kappa-1)}. \tag{2}$$

Eventually, in the lower-tier, the representative household purchase varieties of each good g from different origin countries according to a CES function with elasticity of substitution σ_g and exogenous demand shifters b_{ni}^g:

$$C_{fi}^g = \left[\sum_{n \in \mathcal{I}} (\beta_{ni}^g)^{1/\sigma_g} \left(C_{nfi}^g \right)^{(\sigma_g - 1)/\sigma_g} \right]^{\sigma_g/(\sigma_g - 1)}. \tag{3}$$

2.1.2 Technology

Crop production. Each plot ω is initially covered of natural habitat for wildlife that is unsuitable for crop production. I assume that farmers must pay a fixed cost $z_{fi}^0(\omega)$ in units of the outside good to convert their plot for agricultural use. They then choose which crop $k \in \mathcal{K}^c$ to grow and which technology $\tau \in \mathcal{T}$ to use on that plot. By combining land $L_{fi}^{k\tau}(\omega)$, labor $N_{fi}^{k\tau}(\omega)$ and intermediates $M_{fi}^{k\tau}(\omega)$, the farmer of plot ω can produce:

$$Q_{fi}^{k\tau}(\omega) = \left[\frac{1}{\gamma_L^{k\tau}} z_{fi}^{k\tau}(\omega) L_{fi}^{k\tau}(\omega) \right]^{\gamma_L^{k\tau}} \left[\frac{1}{\gamma_N^{k\tau}} N_{fi}^{k\tau}(\omega) \right]^{\gamma_N^{k\tau}} \left[\frac{1}{\gamma_M^{k\tau}} M_{fi}^{k\tau}(\omega) \right]^{\gamma_M^{k\tau}} \tag{4}$$

where $z_{fi}^{k\tau}(\omega)$ is the productivity of land for the crop-technology pair (k, τ) in plot ω. The technology can be either traditional, $\tau = 0$, or modern, $\tau = 1$, and is characterized by intensity parameters $\gamma_L^{k\tau} \in [0, 1]$, $\gamma_N^{k\tau} \in [0, 1]$ and $\gamma_M^{k\tau} = 1 - \gamma_L^{k\tau} - \gamma_N^{k\tau} \in [0, 1]$. Traditional technology is assumed to use only land and labour (i.e. $\gamma_M^0 = 0$), whereas modern technology uses all three factors.

The bundle of intermediates $M_{fi}^{k\tau}(\omega)$ is a Cobb-Douglas combination of agricultural inputs j:

$$M_{fi}^{k\tau}(\omega) = \prod_{j \in \mathcal{J}} \left(M_{fi}^{k\tau j}(\omega) \right)^{\gamma_M^{kj}}, \tag{5}$$

where $M_{fi}^{k\tau j}(\omega)$ denotes the use of agricultural input j. The intensity parameters $\gamma_M^{kj} \in [0, 1]$ satisfy $\sum_{j \in \mathcal{J}} \gamma_M^{kj} = 1$. Farmers can buy agricultural inputs from different origins according to CES preferences with elasticity of substitution σ_j and exogenous demand shifters b_{ni}^j:

$$M_{fi}^{k\tau j}(\omega) = \left[\sum_{n \in \mathcal{I}} \left(\beta_{ni}^j \right)^{1/\sigma_j} \left(M_{nfi}^{k\tau j}(\omega) \right)^{(\sigma_j - 1)/\sigma_j} \right]^{\sigma_j/(\sigma_j - 1)}. \tag{6}$$

In each plot, the required fixed cost $z_{fi}^0(\omega)$ and land productivities $z_{fi}^{k\tau}(\omega)$ are drawn from field-specific nested Fréchet distributions:

$$\Pr\left(z_{fi}^0(\omega) \leq z_{fi}^0 \right) = \exp\left\{ -\bar{\phi} \left(\frac{z_{fi}^0}{a_{fi}^0} \right)^{-\theta_1} \right\}, \tag{7}$$

$$\Pr\left(z_{fi}^{k\tau}(\omega) \leq z_{fi}^{k\tau}\right) = \exp\left\{-\bar{\phi}\left[\sum_{\tau\in\mathcal{T}}\left(\frac{z_{fi}^{k\tau}}{a_{fi}^{k\tau}}\right)^{-\theta_2}\right]^{\theta_1/\theta_2}\right\} \quad \forall k \in \mathcal{K}^c, \tag{8}$$

where $\bar{\phi} \equiv [\Gamma(1-1/\theta_1)]^{-\theta_1}$ is a constant set to ensure that $\mathbb{E}[z_{fi}^0] = a_{fi}^0$ and $\mathbb{E}[z_{fi}^{k\tau}] = a_{fi}^{k\tau}$. The parameters θ_1 and θ_2 control the heterogeneity of land productivity draws across crops and across technologies within each crop respectively.

Livestock production. The livestock product $k = \ell$ is produced using labor N_i^ℓ and feed-mix F_i:

$$Q_i^\ell = \left[\frac{1}{\gamma_N^\ell} N_i^\ell\right]^{\gamma_N^\ell}\left[\frac{1}{\gamma_F^\ell} F_i\right]^{\gamma_F^\ell} \tag{9}$$

where $\gamma_N^\ell \in [0,1]$ and $\gamma_F^\ell = 1 - \gamma_N^\ell \in [0,1]$ are intensity parameters.[1] Livestock producers choose which crops to put in the feed-mix F_i according to CES preferences with elasticity of substitution ζ and exogenous technological shifters $b_i^{k,feed}$:

$$F_i = \left[\sum_{k\in\mathcal{K}^c}\left(\beta_i^{k,feed}\right)^{1/\zeta}\left(F_i^k\right)^{(\zeta-1)/\zeta}\right]^{\zeta/(\zeta-1)} \tag{10}$$

where F_i^k is the demand for crop k in the feed-mix, which on its turn aggregates over all varieties of crop k. I assume that the preferences of livestock producers over crop origins are similar to those of the representative household:

$$F_i^k = \left[\sum_{n\in\mathcal{I}}\left(\beta_{ni}^k\right)^{1/\sigma_k}\left(F_{ni}^k\right)^{(\sigma_k-1)/\sigma_k}\right]^{\sigma_k/(\sigma_k-1)} \quad \forall k \in \mathcal{K}^a. \tag{11}$$

Assuming that grass cannot be traded implies that livestock producers only buy domestic grass, i.e. $F_i^{grass} = F_{ii}^{grass}$.

Other productions. All other sectors work as in Farrokhi and Pellegrina (2023). Processed fertilizers, denoted $v \in \mathcal{J}$, are produced using the domestic supply of raw fertilizers: $Q_i^v = V_i$. The outside good $g = 0$ and nonfertilizer agricultural inputs $j \in \mathcal{J} \setminus v$ are produced under constant returns to scale using labor only: $Q_i^g = A_i^g N_i^g$, with labor productivity A_i^g.

[1] Contrary to Gouel and Laborde (2021), I do not assume that labor and feed are perfect complements, which simplifies the calibration. They assume that $Q_i^\ell = \min\left(F_i/\mu_i, N_i^\ell/\nu_i^\ell\right)$, where μ_i corresponds to the feed conversion ratio and ν_i^ℓ to the unit labor requirement in country i. In the absence of estimates for the two parameters, I choose to rely on a standard Cobb-Douglas production function. Based on this assumption, I only require data on the cost shares of the two factors.

2.1.3 Labor market

Workers are mobile between sectors but immobile between countries. Each worker φ in country i is endowed with efficiency units $\epsilon_i^s(\varphi)$ for each sector s drawn from Fréchet distribution:

$$\Pr(\epsilon_i^s(\varphi) \leq \epsilon) = \exp\left\{-\left[\Gamma(1-1/\psi)\right]^{-\psi}\left(\frac{\epsilon}{g_i^s}\right)^{-\psi}\right\} \tag{12}$$

where ψ is between-sector labor supply elasticity, and g_i^s is a scale parameter. Workers can supply their efficiency units either to the non-crop sector ($s = 0$) for wage w_i^0 or to the crop sector ($s = 1$) for wage w_i^1, according to which yields the highest revenue $w_i^s \epsilon_i^s(\varphi)$.

2.1.4 Trade system

Goods are traded across fields via a *hub-and-spoke* system, subject to iceberg trade costs: $d_{fif'n}^g \geq 1$ units of g must be shipped from field f in country i to field f' in country n to sell 1 unit. This trade cost can be decomposed as:

$$d_{fif'n}^g = d_{fi}^g \times d_{in}^g \times d_{f'n}^g \tag{13}$$

where d_{fi}^g is the domestic trade cost between field f and its nearest hub in origin country i, d_{in}^g is the hub-to-hub international trade cost, and $d_{f'n}^g$ is the domestic trade cost between field f' and its nearest hub in destination country n. I make three assumptions regarding domestic trade costs. First, the outside good and the livestock product are not subject to any domestic trade costs, i.e. $d_{fif'n}^0 = d_{in}^0$ and $d_{fif'n}^\ell = d_{in}^\ell$. Second, agricultural inputs are not subject to domestic trade costs in the origin country, i.e. $d_{fif'n}^j = d_{in}^j \times d_{f'n}^j$. Third, crops are not subject to domestic trade costs in the destination country, i.e. $d_{fif'n}^j = d_{fi}^j \times d_{in}^j$. As such, everything works as if all goods but crops were produced in hubs, and all goods but agricultural inputs were consumed in hubs. Similarly, w_i^0 can be interpreted as a *urban* wage and w_i^1 as a *rural* wage.

Goods are not differentiated by fields or hubs. As a result, producer prices including domestic trade costs must be equalized in origin country i, i.e. $p_{fi}^k d_{fi}^k = p_i^k$; producers in more remote fields receive a lower price for crop k. Consumer prices including domestic trade costs must also be equalized in destination country n, i.e. $p_{f'n}^j = p_{in}^j d_{in}^j$; consumers in more remote fields pay a higher price for agricultural input j.

2.1.5 Biodiversity

Land can be categorized as either natural habitat or agricultural.[2] I then decompose *current* land-use in ecoregion e as:

$$L_e = L_e^{nat} + \sum_k \sum_\tau L_e^{k\tau} \tag{14}$$

where $L_e^{nat} = \sum_{f \in \mathcal{F}_e} L_{fe}^{nat}$ is the remaining natural habitat area and $L_e^{k\tau} = \sum_{f \in \mathcal{F}_e} L_{fe}^{k\tau}$ is the area dedicated to the crop-technology pair (k, τ) in ecoregion e.

Species richness. Given this distribution of land, the Countryside Species-Area model (Pereira and Daily, 2006) can be used to estimate a species extinction rate, s_e^{lost}, in every ecoregion e:

$$s_e^{lost} = 1 - \left(\frac{L_e^{nat} + \sum_k \sum_\tau h_e^{k\tau} \times L_e^{k\tau}}{L_e} \right)^{z_e}. \tag{15}$$

Crucially, the relationship accounts for birds' affinity for each type-intensity pair (k, τ) of agricultural land-use through parameters $h_e^{k\tau} \in [0, 1]$. It is assumed that $h_e^{nat} = 1$ —natural habitat can support all bird species—and that affinity decreases as land-use becomes increasingly hostile for birds. For example, it is reasonable to assume that the survival rate of birds is lower in modern agricultural areas than in traditional ones. Prior to any alteration in land-use, I assume that every ecoregion consisted solely of natural habitats and was home to a number S_e^0 of bird species. Using Eq. (15), I can predict the number of bird species committed to extinction in the medium- to long-term in ecoregion e:

$$S_e^{lost} = \sum_k \sum_\tau \underbrace{\frac{L_e^{k\tau}\left(1 - h_e^{k\tau}\right)}{\sum_k \sum_\tau \left[L_e^{k\tau}(1 - h_e^{k\tau})\right]} \frac{1}{L_e^{k\tau}} s_e^{lost}}_{CF_e^{k\tau}} S_e^0 L_e^{k\tau} \tag{16}$$

where $CF_e^{k\tau}$, referred to as *characterization factors* in the ecology literature, measure the regional species loss per m^2 of land-use (k, τ).

Abundance. I assume that population follows a Verhulst logistic growth model:

$$A_e^b(t+1) = A_e^b(t) \left[1 + r^b - r^b \frac{A_e^b(t)}{K_e^b(t)} \right] \tag{17}$$

The number of individuals of species b in ecoregion e at time $t+1$, $A_e^b(t+1)$, therefore depends on (1) the population size in the previous year, $A_e^b(t)$; (2) a specific natural growth

[2] I exclude other human-modified land categories, such as urban areas, which are quantitatively negligible relative to agricultural areas.

rate—essentially related to the number of eggs a female can lay without environmental pressure—, r^b; and (3) the carrying capacity of regional ecosystem e for species b in year t, $K_e^b(t)$. The carrying capacity refers to the maximum number of individuals of species b the habitat can sustain, given current ecological conditions. I assume that it is a function of land-use surfaces, $L_e^k(t)$, and climate, $Climate_e(t)$. I consider further that $K_e^b(t)$ directly depends on the total quantity of each agricultural input j used in the ecoregion, $M_e^j(t)$. Thus,

$$\frac{1}{K_{fi}^b(t)} = \iota^b + \sum_{k \in \mathcal{K}^c} \iota_k^b L_e^k(t) + \sum_{j \in \mathcal{J}} \iota_j^b M_e^j(t) + \iota_{\text{clim}}^b Climate_e(t), \tag{18}$$

where ι^b is species fixed effect, ι_k^b assesses the response of species b to land-use k, ι_j^b to the use of input j, and ι_{clim}^b to climate conditions.

2.2 General equilibrium

2.2.1 Good demand

Given equations (1), (2), (3) and (13), utility maximization by the representative household in (f, i) requires

$$C_{fi}^1 = \left(\frac{P_{fi}^a}{P_{fi}}\right)^{-\eta} \beta_i^1 C_{fi}, \tag{19}$$

$$C_{fi}^k = \left(\frac{P_{fi}^k}{P_{fi}^a}\right)^{-\kappa} \beta_i^k C_{fi}^1, \tag{20}$$

and

$$C_{nfi}^g = \left(\frac{p_n^g d_{ni}^g d_{fi}^g}{P_{fi}^g}\right)^{-\sigma_g} \beta_{ni}^g C_{fi}^g. \tag{21}$$

Price indexes that enter the above tiers are:

$$P_{fi} = \left[\beta_i^0 (P_{fi}^0)^{1-\eta} + \beta_i^1 (P_{fi}^1)^{1-\eta}\right]^{\frac{1}{1-\eta}}, \tag{22}$$

$$P_{fi}^1 = \left[\sum_{k \in \mathcal{K}} \beta_i^k (P_{fi}^k)^{1-\kappa}\right]^{\frac{1}{1-\kappa}}, \tag{23}$$

and

$$P_{fi}^g = \left[\sum_{n \in \mathcal{I}} \beta_{ni}^g (p_n^g d_{ni}^g d_{fi}^g)^{1-\sigma_g}\right]^{\frac{1}{1-\sigma_g}}. \tag{24}$$

Given assumptions on domestic trade costs, $P_{fi}^g = P_i^g = \left[\sum_{n\in\mathcal{I}} \beta_{ni}^g (p_n^g d_{ni}^g)^{1-\sigma_g}\right]^{\frac{1}{1-\sigma_g}}$ for $g = 0$ and $g \in \mathcal{K}^a$, and for all fields $f \in \mathcal{F}_i$.

2.2.2 Production

Crop production. The marginal cost of crop k using technology τ in plot ω of (f,i), $c_{fi}^{k\tau}(\omega)$, is

$$c_{fi}^{k\tau}(\omega) = \left(\frac{r_{fi}^{k\tau}(\omega)}{z_{fi}^{k\tau}(\omega)}\right)^{\gamma_L^{k\tau}} \left(w_i^1\right)^{\gamma_N^{k\tau}} \left(m_{fi}\right)^{\gamma_M^{k\tau}}$$

where $r_{fi}^{k\tau}(\omega)$ is the gross rental price of plot ω and $m_{fi} \equiv \prod_{j\in\mathcal{J}} \left(P_{fi}^j\right)^{\gamma_M^{kj}}$ is the price index of the bundle of agricultural inputs in destination (f,i). Perfect competition in the crop market implies $c_{fi}^{k\tau}(\omega) = p_{fi}^k$. Thus, as shown in Farrokhi and Pellegrina (2023),

$$r_{fi}^{k\tau}(\omega) = z_{fi}^{k\tau}(\omega) h_{fi}^{k\tau} \tag{25}$$

with

$$h_{fi}^{k\tau} \equiv p_{fi}^k \underbrace{\left(\frac{w_i^1}{p_{fi}^k}\right)^{-\gamma_N^{k\tau}/\gamma_L^{k\tau}} \left(\frac{m_{fi}}{p_{fi}^k}\right)^{-\gamma_M^{k\tau}/\gamma_L^{k\tau}}}_{\equiv \tilde{h}_{fi}^{k\tau}}$$

summarizing market prices effects. In equilibrium, the land share of the crop-technology pair (k,τ) in (f,i), $\pi_{fi}^{k\tau}$, is

$$\pi_{fi}^{k\tau} = \alpha_{fi}^k \times \alpha_{fi}^{k\tau} \tag{26}$$

where

$$\alpha_{fi}^{k\tau} = \frac{\left(a_{fi}^{k\tau} h_{fi}^{k\tau}\right)^{\theta_2}}{\left(H_{fi}^k\right)^{\theta_2}} \tag{27}$$

is the share of land within crop k allocated to technology τ, and

$$\alpha_{fi}^k = \frac{\left(H_{fi}^k\right)^{\theta_1}}{(a_{fi}^0 P_{fi}^0)^{\theta_1} + \sum_{k\in\mathcal{K}^c} \left(H_{fi}^k\right)^{\theta_1}} \tag{28}$$

is the share of land allocated to crop k. The term H_{fi}^{k} denotes the aggregate return to crop k:

$$H_{fi}^{k}=\left[\sum_{\tau\in\mathcal{T}}\left(a_{fi}^{k\tau}h_{fi}^{k\tau}\right)^{\theta_2}\right]^{1/\theta_2}. \tag{29}$$

Let $\Omega_{fi}^{k\tau}$ be the set of plots ω in field f to which crop-technology (k,τ) is optimally allocated. Combining Eq. (25)-(29), production of (k,τ) in plot ω is given by

$$Q_{fi}^{k\tau}(\omega)=\begin{cases}\left(\gamma_{L}^{k\tau}\right)^{-1}\tilde{h}_{fi}^{k\tau}z_{fi}^{k\tau}(\omega),\ \omega\in\Omega_{fi}^{k\tau}\\ 0,\ \omega\notin\Omega_{fi}^{k\tau},\end{cases} \tag{30}$$

and at the field level by

$$Q_{fi}^{k\tau}=L_{fi}\left(\gamma_{L}^{k\tau}\right)^{-1}\tilde{h}_{fi}^{k\tau}a_{fi}^{k\tau}\left(\alpha_{fi}^{k}\right)^{(\theta_1-1)/\theta_1}\left(\alpha_{fi}^{k\tau}\right)^{(\theta_2-1)/\theta_2}. \tag{31}$$

Aggregate output of crop k, Q_{i}^{k} at the location of hubs in country i is

$$Q_{i}^{k}=\sum_{\tau\in\mathcal{T}}Q_{i}^{k\tau} \tag{32}$$

with

$$Q_{i}^{k\tau}=\sum_{f\in\mathcal{F}_i}\frac{Q_{fi}^{k\tau}}{d_{fi}^{k}}. \tag{33}$$

Lastly, the quantity of outside good required for setting up land in country i, FC_{i}^{0}, equals

$$FC_{i}^{0}=\sum_{f\in\mathcal{F}_i}L_{fi}a_{fi}^{0}\left[1-\left(1-\sum_{k\in\mathcal{K}^c}\alpha_{fi}^{k}\right)^{(\theta_1-1)/\theta_1}\right]. \tag{34}$$

Livestock production. The share of crop k in the feed-mix of country i is

$$\frac{F_{i}^{k}}{F_{i}}=\beta_{i}^{k,feed}\left(\frac{P_{i}^{feed}}{P_{i}^{k}}\right)^{-\zeta} \tag{35}$$

with

$$P_{i}^{feed}=\left[\sum_{k\in\mathcal{K}^c}\beta_{i}^{k,feed}(P_{i}^{k})^{1-\zeta}\right]^{\frac{1}{1-\zeta}}. \tag{36}$$

Perfect competition in the livestock sector then implies

$$c_i^\ell = \left(w_i^1\right)^{\gamma_\ell^N} \left(P_i^{feed}\right)^{\gamma_\ell^F} = p_i^\ell. \tag{37}$$

2.2.3 Labor supply

The share of labor supply in sector s, n_i^s, equals

$$n_i^s = \frac{N_i^s}{N_i} = \frac{\left(g_i^s w_i^s\right)^\psi}{\sum_{s\in\{0,1\}} \left(g_i^s w_i^s\right)^\psi} \tag{38}$$

and aggregate supply of efficiency units to sector s, $\tilde{N}_i^s$, is

$$\tilde{N}_i^s = g_i^s \left(n_i^s\right)^{(\psi-1)/\psi} N_i. \tag{39}$$

2.2.4 International trade

Total import demand for crop $k \in \mathcal{K}^c$ in country i is the sum of demand for final consumption and for feed-mix

$$\frac{X_i^k}{P_i^k} = C_i^k + F_i^k \tag{40}$$

where X_i^k is the total value of imports. The share of good g from origin n in total imports value of destination (f,i) is

$$\frac{X_{nfi}^g}{X_{fi}^g} = \beta_{ni}^g \left(\frac{p_n^g d_{ni}^g d_{fi}^g}{P_{fi}^g}\right)^{1-\sigma_g}. \tag{41}$$

Given assumptions on internal trade costs, we observe that for $g = 0$ and $g \in \mathcal{K}^a$, $\frac{X_{nfi}^g}{X_{fi}^g} = \frac{X_{ni}^g}{X_i^g}$ for all fields $f \in \mathcal{F}_i$.

2.2.5 Market clearing conditions

The goods market clears for the outside good $g = 0$, agricultural inputs $j \in \mathcal{J}$, grass and other agricultural outputs $k \in \mathcal{K}^a$ when supply in the origin country n equals world demand:

$$p_n^0 Q_n^0 = \sum_{i\in\mathcal{I}} X_{ni}^0 + P_n^0 L_n^0, \tag{42}$$

$$p_n^j Q_n^j = \sum_{i\in\mathcal{I}} \sum_{f\in\mathcal{F}_i} \sum_{k\in\mathcal{K}^c} \beta_{ni}^j \left(\frac{p_n^j d_{ni}^j}{P_i^j}\right)^{-\zeta} \gamma_{Mj}^k \gamma_M^{k1} p_i^k Q_{fi}^{k1}, \tag{43}$$

$$p_n^{grass} Q_n^{grass} = \beta_i^{grass,feed} \left(\frac{p_i^{grass}}{P_i^{feed}} \right)^{-\zeta} \gamma_F^{\ell} p_n^{\ell} Q_n^{\ell}, \tag{44}$$

$$p_n^k Q_n^k = \sum_{i \in \mathcal{I}} \left(\frac{p_n^k d_{ni}^k}{P_i^k} \right)^{-\sigma_k} \beta_{ni}^k \left(\beta_i^k \beta_i^a E_i + \beta_i^{k,feed} \left(\frac{P_i^k}{P_i^{feed}} \right)^{-\zeta} \gamma_F^{\ell} p_n^{\ell} Q_n^{\ell} \right) \quad \forall k \in \mathcal{K}^a. \tag{45}$$

Labor market clearing in every country i requires that labor supply in each sector equal their corresponding labor demand:

$$w_i^0 \tilde{N}_i^0 = \gamma_N^{\ell} p_i^{\ell} Q_i^{\ell} + p_i^0 Q_i^0 + \sum_{j \in \mathcal{J}, k \neq v} p_i^j Q_i^j, \tag{46}$$

$$w_i^1 \tilde{N}_i^1 = \sum_{k \in \mathcal{K}^c} \sum_{\tau \in \mathcal{T}} \gamma_N^{k\tau} p_i^k Q_i^{k\tau}. \tag{47}$$

2.2.6 Expenditures

Total expenditure in country i, E_i, equals the sum of factor rewards

$$E_i = w_i^0 \tilde{N}_i^0 + w_i^1 \tilde{N}_i^1 + R_i + p_i^v V_i. \tag{48}$$

where R_i denotes aggregate net land rents in country i.

2.2.7 Definition

Definition 1. For all countries $i, n \in \mathcal{I}$, ecoregions $e \in \mathcal{E}$, fields $f \in \mathcal{F}_i$, goods $g \in \mathcal{G}$ consisting of an outside good, agricultural inputs $j \in \mathcal{J}$, agricultural outputs $k \in \mathcal{K}$, sectors $s \in \{0, 1\}$, and technologies $t \in \mathcal{T}$, a global economy is characterized by endowments $\mathcal{D} \equiv \{L_{fi}, N_i, V_i, L_e, S_e^0\}$, supply parameters $\Omega_S \equiv \{\theta_1, \theta_2, \varphi, g_i^s, \gamma_L^{k\tau}, \gamma_M^{k\tau}, \gamma_N^{k\tau}, \gamma_{Mj}^k, a_{fi}^0, a_{fi}^{k\tau}\}$, and demand parameters $\Omega_D \equiv \{\eta, \kappa, \sigma_g, \beta_i^0, \beta_i^1, \beta_i^k, \beta_i^{k,feed}, \beta_{ni}^k, d_{ni}^k, d_{fi}^k, A_i^k\}$.

Definition 2. Given a global economy characterized by $\{\mathcal{D}, \Omega_S, \Omega_D\}$ a general equilibrium consists of prices $\{p_i^g\}$ in all countries $i \in \mathcal{I}$ and for all goods $g \in \mathcal{G}$, such that equations (19)-(48) hold.

3 Estimation

In order to simulate the model described in the previous section, data on endowments, as well as estimates of the demand, supply and ecological parameters, are required. In this section, I present the data used and the methods employed to estimate the parameters missing from the literature. Eventually, I evaluate the model's fit.

3.1 Data

The model is calibrated at three spatial scales—countries, ecoregions, and individual fields. The species-richness component is calibrated across global ecoregions, while the abundance component uses finer-resolution U.S. Level-IV ecoregions. The dataset includes 66 countries (with one representative for the rest of the world), 698 world ecoregions, 393 U.S. Level-IV ecoregions, and 822,053 fields. It covers 36 agricultural outputs (including a livestock aggregate) and three agricultural inputs: pesticides, fertilizers, and farm machinery. I choose 2011 as the baseline year.

Country-level data. For the outside good, agricultural inputs and the agricultural output sector as a whole, I use data on bilateral trade flows and gross outputs built by Farrokhi and Pellegrina (2023) using information from BACI-CEPII, FAOSTAT, WIOD, OECD IOTs, STAN and UNIDO. I also collect data on bilateral trade flows, production weight, production value, land-use, and producer prices for each agricultural output (but grass) from FAOSTAT. Data for the livestock good are derived by aggregating data on meat, eggs, milk and dairy products. The demand of a crop for feed is calculated using FAOSTAT Food Balance Sheets. Eventually, the value of grass production and grass price are computed by combining FAOSTAT data on land-use with data on the value added accruing to land for "Bovine cattle, sheep and goats, horses", "Animal products nec" and "Raw milk" from the GTAP database version 9.2.

Global ecoregion-level data. Global ecoregions are defined by WWF as "large unit of land or water containing a geographically distinct assemblage of species, natural communities, and environmental conditions". I recover the boundaries of each ecoregion from Olson et al. (2001) and the original number of bird species, S_e^0, from Chaudhary and Brooks (2018). My field selection covers on average 66% of an ecoregion area. The original number of birds species varies from 24 to 847, with significant spatial disparities between the northern and the southern hemispheres. I rely on Scherer et al. (2023) for characterization factors, $CF_e^{k\tau}$. Among available type-intensity pairs of land-use, I select the following: cropland minimal, cropland intensive, plantation minimal, plantation intensive, and pasture minimal. I assume that the 'minimal' intensity corresponds to the traditional technology $\tau = 0$ in my model, and 'intensive' to the modern technology $\tau = 1$. I assume further that all crops but palm and grass belong to the type 'cropland', while palm belongs to the type 'plantation' and grass corresponds to 'pasture'.

US ecoregion-level data. To calibrate the population-dynamics model I require fine-scale data on bird abundance, land-use practices, input applications, and climate. Such high-resolution datasets are uniquely available for the United States. For bird abundance I rely on the North American Breeding Bird Survey (NABBS), a long-term, continent-wide monitoring program

(Pardieck et al., 2020). NABBS follows a strict, repeatable protocol that yields high-quality trend data: each year, trained volunteers drive predetermined 40km routes, stopping at 50 points per route. At each stop they record all birds seen or heard within a 400m radius. This standardized effort provides consistent, comparable counts across years and regions. Data are available at the species-route-segment-year combination, covering more than 400 bird species on thousands of routes (see Figure A.1 for a map). I select the 100 most abundant bird species in 1992. Land-use information comes from an ESA satellite product that classifies every $0.002^\circ \times 0.002^\circ$ pixel, notably distinguishing between cropland and pasture (cropland pixels are depicted in Figure A.1). To account for local climate, I then collect data on monthly precipitation and temperature from an ESA reanalysis provided on a $0.25^\circ \times 0.025^\circ$ grid, which I aggregate at the seasonal level. Eventually, I use pesticide-application totals from the U.S. Geological Survey reported at the county level. All of these variables are aggregated to the Level-IV ecoregion level by intersecting each original spatial unit with ecoregion boundaries and applying the same area-based weight—the proportion of the unit's area that lies within the ecoregion—to either sum (for bird counts, cropland and pasture area) or average (for climate variables and pesticide use). Overall, the resulting sample spans the years 1992 through 2017.

Field-level data. Potential yields are sourced from the Global Agro-Ecological Zoning (GAEZ) project (Fischer et al., 2021). GAEZ agronomic model produces field-level yield estimates by evaluating each field's edaphic and climatic attributes—including dominant soil type, altitude, slope, temperature, precipitation, and related variables—against the specific requirements of individual crops. In this framework a 'field' corresponds to a 5'×5' grid cell, which approximates an area of 10km×10km. As is common in the literature, I select the estimates for the reference period 1961-1990 under rain-fed conditions. GAEZ also provides yields for different levels of input use. I map these input regimes onto the technology parameter τ in my model: the low-input regime, representing conventional, subsistence-oriented land management, corresponds to $\tau = 0$ (traditional); the high-input regime, reflecting intensive, market-oriented management with fertilizer, irrigation, and mechanization, corresponds to $\tau = 1$ (modern). To anchor the model in observed land-use patterns, I also use data on the proportions of each field occupied by cropland and pasture circa 2000 from Earthstat (Ramankutty et al., 2008). These figures are derived from a synthesis of national agricultural inventories and satellite-derived land-cover maps.

3.2 Demand-side parameters

The demand-side parameters are estimated directly from the model's micro-foundations, closely following Farrokhi and Pellegrina (2023), and are summarized in Table 1.

Lower-tier demand for agricultural outputs. Based on Eq. (41), I first estimate the elasticity of substitution between crop-varieties σ_k using:

$$\log\left(\frac{X_{ni}^k}{X_i^k}\right) = \delta_i^k + (1-\sigma_k)\log p_n^k + \epsilon_{ni}^k$$

where $\delta_i^k \equiv -\log\left[\sum_{n\in\mathcal{I}} \beta_{ni}^k (p_n^k d_{ni}^k)^{1-\sigma_k}\right]$ is an importer-crop fixed effect and $\epsilon_{ni}^k \equiv \log\left[\beta_{ni}^k \left(d_{ni}^k\right)^{1-\sigma_k}\right]$ is a residual. Setting $\sum_{n\in\mathcal{I}} \epsilon_{ni}^k = 0$, I estimate $\beta_{ni}^k \left(d_{ni}^k\right)^{1-\sigma_k}$ and a different elasticity of substitution σ_k for cereals, perishables and non-perishables. To account for endogeneity, I compute an average of GAEZ potential yields across fields in the exporting country and use it to intrument $\log p_n^k$.

Lower-tier demand for other goods. Following the literature, I set $\sigma_g = 4$ for the manufacturing good and for agricultural inputs. For $g = \{\text{manufacturing, pesticides, machinery}\}$, I estimate:

$$\log\left(\frac{X_{ni}^g}{X_i^g}\right) - (1-\sigma_g)\log w_n = \delta_i^g + \delta_n^g + \epsilon_{ni}^g$$

where $\delta_i^g \equiv (1-\sigma_g)\log P_i^g$ is a destination fixed effect, $\delta_n^g \equiv (1-\sigma_g)\log A_n^g$ is an origin fixed effect and $\epsilon_{ni}^g \equiv \log\left[\beta_{ni}^g \left(d_{ni}^g\right)^{1-\sigma_g}\right]$. This allows to recover $\beta_{ni}^g \left(d_{ni}^g\right)^{1-\sigma_g}$ and A_n^g. For $g = \{\text{fertilizers}\}$, I estimate:

$$\log\left(\frac{X_{ni}^g}{X_i^g}\right) - (1-\sigma_g)\log p_i^g = \delta_i^g + \epsilon_{ni}^g$$

and recover $\beta_{ni}^g \left(d_{ni}^g\right)^{1-\sigma_g}$ from residuals.

Middle-tier demand for agricultural outputs. Based on Eq. (20), I then estimate the elasticity of substitution between agricultural outputs κ using:

$$\log\left(\frac{X_i^k}{X_i^1}\right) = \delta_i + (1-\kappa)\log P_i^k + \epsilon_i^k$$

where $\delta_i \equiv (1-\kappa)\log P_i^1$ is a country fixed effect and $\epsilon_i^k \equiv \log \beta_i^k$ is a residual. I assume, without loss of generality, that $\sum_{k\in\mathcal{K}^a} \epsilon_i^k = 0$. P_i^k is constructed using the estimates of σ_k and $\beta_{ni}^k \left(d_{ni}^k\right)^{1-\sigma_k}$ from the previous step following Eq. (24). I address potential endogenity issues by instrumenting $\log P_i^k$ using the average of GAEZ potentiel yield acros fields for crop k in country i. The procedure also allows to recover β_i^k from the residuals.

Upper-tier demand. I borrow from Comin, Lashkari, and Mestieri (2021) and set the elasticity of substitution between agricultural and non-agricultural goods to $\eta = 0.5$. Given this estimate, I recover β_i^0 and β_i^1 based on Eq. (19) and Eq. (22).

Table 1: Demand-side parameters

Parameters	Description	Source	Estimate
σ_k for cereals	Elast. of subst. between varieties	Estimated from gravity eq.	9.19 (3.78)
σ_k for perishables	Elast. of subst. between varieties	Estimated from gravity eq.	2.96 (0.74)
σ_k for non-perishables	Elast. of subst. between varieties	Estimated from gravity eq.	5.87 (0.56)
σ_g for $g = 0$, $g \in \mathcal{J}$	Elast. of subst. between varieties	Literature	4
κ	Elast. of subst. between ag. outputs	Estimated from gravity eq.	1.25 (0.11)
η	Elast. of subst. between ag. and non-ag.	Comin, Lashkari, and Mestieri (2021)	0.5
$b_{ni}^k (d_{ni}^k)^{1-\sigma_k}$, b_i^k	Demand shifters of ag. outputs	Residuals from gravity eq.	–
$b_{ni}^g (d_{ni}^g)^{1-\sigma_g}$, $g \neq k$	Demand shifters of other goods	Farrokhi and Pellegrina (2023)	–
b_i^0, b_i^1	Demand shifters of sectors	Farrokhi and Pellegrina (2023)	–
d_{fi}^g	Domestic trade costs	Farrokhi and Pellegrina (2023)	–
$b_i^{k,feed}$	Demand shifters of crops in feed	Residuals from FE reg.	–

Notes: The table presents sources and estimation methods for the structural demand-side parameters of the model. Standard errors are clustered at the country of origin and good level.

Middle-tier demand for feed. I set the elasticity of substitution between crops in the feed mix to $\zeta = 0.9$, as in Gouel and Laborde (2021). Based on Eq. (35), I then estimate feed demand shifters $\beta_i^{k,feed}$ using:

$$\log F_i^k + \zeta P_i^k = \delta_i^{feed} + \epsilon_i^{k,feed}$$

where $\delta_i^{feed} \equiv \log F_i - \zeta \log P_i^{feed}$ is a country fixed effect and $\epsilon_i^{feed,k} \equiv \log \beta_i^{k,feed}$ is a residual.

3.3 Supply-side parameters

I adopt most of the supply-side parameters from Farrokhi and Pellegrina (2023). The factor- and input-share values are taken as constant across all crops (with the exception of grass in my case, which uses only land). Accordingly, I set: $\gamma_L^{k1} = 0.206$, $\gamma_N^{k1} = 0.207$, $\gamma_M^{k1} = 0.587$ for the modern technology; $\gamma_L^{k0} = 0.551$, $\gamma_N^{k0} = 0.449$ and $\gamma_M^{k0} = 0$ for the traditional technology; $\gamma_M^{fertilizers} = 0.256$, $\gamma_M^{pesticides} = 0.158$ and $\gamma_M^{machinery} = 0.585$ for agricultural input shares within the modern technology. I also set the elasticity of production choices between crops to $\theta_1 = 1.38$ and the elasticity of production choices between technologies to $\theta_2 = 4.51$. Crop-technology productivity shifters are recovered using GAEZ data on potential yields, following the methdology described in Farrokhi and Pellegrina (2023). For livestock

Table 2: Supply-side parameters

Parameters	Description	Source	Value
θ_1	Productivity dispersion betw. crops	Farrokhi and Pellegrina (2023)	1.38
θ_2	Productivity dispersion betw. technologies	Farrokhi and Pellegrina (2023)	4.51
ζ	Elast. of subst. betw. crops in feed	Gouel and Laborde (2021)	0.9
$a_{fi}^{k\tau}$	Crop-technology productivity shifter	Potential yields from FAO-GAEZ	–
a_{fi}^{0}	Investment intensity parameter	Farmland shares from EarthStat	–
A_i^0, A_i^j	Productivity shifters of non-crop goods	Farrokhi and Pellegrina (2023)	–
$\gamma_L^{k\tau}$, $\gamma_N^{k\tau}$, $\gamma_M^{k\tau}$	Crop factor shares	Farrokhi and Pellegrina (2023)	–
γ_M^{kj}	Crop input shares	Farrokhi and Pellegrina (2023)	–
γ_N^{ℓ}, γ_F^{ℓ}	Livestock factor shares	Cost shares from USDA	–
ψ	Between-sector labor supply elasticity	Literature	2

Notes: The table presents sources for the structural supply-side parameters of the model.

production, labor- and feed-share parameters are calibrated to USDA-reported cost shares, i.e. $\gamma_N^{\ell} = 0.38$ and $\gamma_F^{\ell} = 0.62$, while the elasticity of substitution among crops in the feed mix borrow from the literature review of Gouel and Laborde (2021), i.e. $\zeta = 0.9$. The source and value (when applicable) of all supply-side parameters is reported in Table 2.

3.4 Ecological parameters

As mentioned earlier, the ecological model for species richness is calibrated using characterization factors taken from Scherer et al. (2023). In contrast, the parameters required for the abundance component are absent from the existing literature. Consequently, I calibrate this part of the model with empirical data on bird abundance, land-use patterns, climate variables, and pesticide application across the United States. Combining Eq. (17) and (18), and adjusting for data limitations, I estimate the following equation for each of the 100 bird species

in my sample:

$$\begin{aligned} A_e^b(t+1) = \alpha_e &+ \beta_s^1 \times A_e^b(t) + \beta_b^2 \times A_e^b(t)^2 + \beta_b^3 \times \text{CROPLAND}_e(t) \times A_e^b(t)^2 \\ &+ \beta_b^4 \times \text{PASTURE}_e(t) \times A_e^b(t)^2 + \beta_b^5 \times \text{PESTICIDES}_e(t) \times A_e^b(t)^2 \\ &+ \beta_b^6 \times \text{TEMP-WINTER}_e(t) \times A_e^b(t)^2 + \beta_b^7 \times \text{TEMP-SPRING}_e(t) \times A_e^b(t)^2 \\ &+ \beta_b^8 \times \text{TEMP-SUMMER}_e(t) \times A_e^b(t)^2 + \beta_b^9 \times \text{TEMP-FALL}_e(t) \times A_e^b(t)^2 \\ &+ \beta_b^{10} \times \text{PRECIP-WINTER}_e(t) \times A_e^b(t)^2 + \beta_b^{11} \times \text{PRECIP-SPRING}_e(t) \times A_e^b(t)^2 \\ &+ \beta_b^{12} \times \text{PRECIP-SUMMER}_e(t) \times A_e^b(t)^2 + \beta_b^{13} \times \text{PRECIP-FALL}_e(t) \times A_e^b(t)^2 \\ &+ \epsilon_e^b \end{aligned} \tag{49}$$

where α_e is a Level-IV ecoregion fixed effects, $\text{CROPLAND}_e(t)$ (resp. $\text{PASTURE}_e(t)$) is the total cropland (resp. pasture) area in ecoregion e in year t, $\text{TEMP-WINTER}_e(t)$ is the mean temperature in ecoregion e during the first quarter of year t—similarly spring corresponds to the second quarter, fall to the third and winter to the fourth–, $\text{PRECIP-WINTER}_e(t)$ corresponds to total precipitation in ecoregion e during the first quarter—with analogous variables for the other seasons— and ϵ_e^b is a residual. The β_b parameters are the species-specific coefficients to be estimated. I do not incorporate crop-specific effects or other agricultural inputs because the requisite data are unavailable. Similarly, I refrain from modelling technological influences beyond the pesticide effect; U.S. agriculture is already largely modernized, making it difficult to disentangle any additional impact of traditional versus modern practices.

A naive OLS estimation of Eq. (49) is likely to suffer from endogeneity: although ecoregion fixed effects absorb time-invariant heterogeneity, land-use decisions and pesticide applications may still be correlated with time-varying unobserved factors—such as local economic shocks, shifts in land management intensity, or changes in environmental policy—that independently affect bird habitat quality. To address this, I construct shift-share (Bartik) instruments that exploit China's accession to the WTO in 2001 as a plausibly exogenous demand shock. For cropland, the instrument interacts ecoregion-level potential yields from FAO-GAEZ—which capture time-invariant agronomic suitability for each crop—with the log change in Chinese agricultural imports of that crop relative to the 1992 baseline, and sums across crops (excluding grass):

$$Z_e^{\text{crop}}(t) = \sum_{k \neq \text{grass}} \text{PotYield}_{ek} \cdot \Delta\text{ChinaImports}_k^{-\text{USA, BRA, ARG}}(t)$$

where PotYield_{ek} is GAEZ potential yields for crop k in ecoregion e, and $\text{ChinaImports}_k(t)$ is log change in Chinese imports of crop k relative to 1992 baseline. For pasture, an analogous

instrument interacts GAEZ grass suitability with the change in Chinese livestock imports:

$$Z_e^{\text{pasture}}(t) = \text{PotYield}_{e,\text{grass}} \cdot \Delta\text{ChinaImports}_{\text{livestock}}^{-\text{USA, BRA, ARG}}(t).$$

For pesticides, the instrument interacts each ecoregion's 1992 share of national pesticide use with the aggregate change in Chinese pesticide imports:

$$Z_e^{\text{pest}}(t) = \text{PestShare}_{e,1992} \cdot \Delta\text{ChinaPestImports}^{-\text{USA, BRA, ARG}}(t).$$

In all three cases, the source countries excluded from the trade shocks are the United States itself, Brazil, and Argentina. The United States is excluded as its own agricultural exports to China are endogenous to the local conditions that also determine bird abundance. Brazil and Argentina are excluded as source countries because they host major wintering grounds for migratory birds that breed in the United States. Including them would violate the exclusion restriction if rising Chinese demand for soybeans triggers cropland expansion in these countries, destroying wintering habitat and reducing the survival of migrants independently of any change in U.S. land use. The resulting instruments vary across both ecoregions (through the exposure component) and time (through the trade-shock component), satisfying the relevance condition while being plausibly excludable from the population-dynamics equation.

A second econometric concern arises because Eq. (49) is a dynamic panel model—current abundance depends on its own lag—estimated with ecoregion fixed effects. As shown by Nickell (1981), the within-group transformation mechanically correlates the demeaned lagged dependent variable with the demeaned error term, biasing the autoregressive coefficient downward and potentially distorting the other estimates. To correct for this, I complement the IV estimates with Arellano–Bond difference GMM (Arellano and Bond, 1991), which eliminates the fixed effects by first-differencing and instruments the lagged dependent variable with its deeper lags.

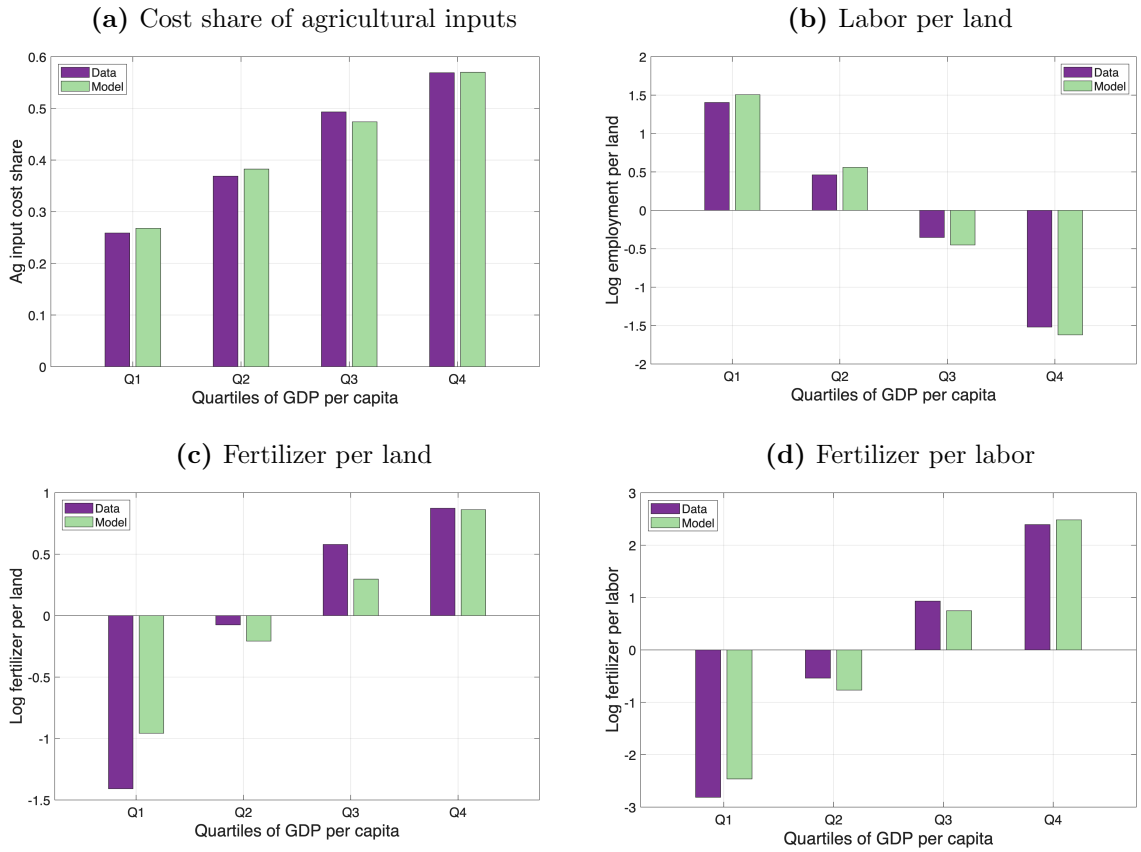
3.5 Other parameters

I consider $d_{fi}^g = d_{fi}$ and take the values of domestic trade costs from Farrokhi and Pellegrina (2023), which were estimated using the methodology of Allen and Arkolakis (2014) and data on the transportation networks of all countries. Following Farrokhi and Pellegrina (2023) again, I set the labor supply elasticity to 2, i.e. $\psi = 2$, and normalize the shifters of labor supply to 1, i.e. $g_i^1 = g_i^0 = 1$.

3.6 Goodness of fit

Land-use. In the current version of this paper, I calibrate the model for 34 crops only, omitting the livestock sector and grass. I evaluate whether the calibrated model reproduces untargeted moments that capture cross-country variation in agricultural input intensity. As

Figure 1: Model fit on measures of input intensity



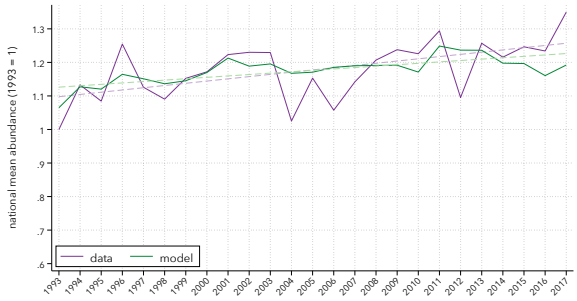
Notes: Each panel in the above figure plots observed (purple bars) and model-predicted (green bars) measures of input intensity for each quartile of GDP per capita. GDP per capita, labor per land, fertilizer per land and fertilizer per labor are normalized according to their global averages.

illustrated in Figure 1, the model provides an excellent fit to the empirical distribution of several key indicators—cost share of agricultural inputs, labor per unit of land, fertilizer per unit of land, and fertilizer per unit of labor—across all quartiles of GDP per capita. I go further and verify that the calibration generates consistent acreage elasticities, which can be computed as:

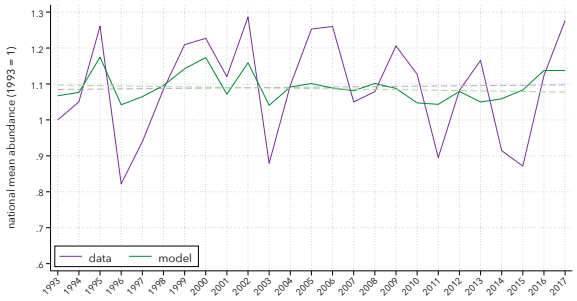
$$\frac{dL_i^k}{dp_i^k}\frac{p_i^k}{L_i^k} = \sum_\tau \sum_f \frac{L_{fi}^{k\tau}}{L_i^k}\frac{1}{\gamma_L^{k\tau}}\left[\theta_1 \alpha_{fi}^{k\tau}(1-\alpha_{fi}^k) + \theta_2(1-\alpha_{fi}^{k\tau})\right].$$

Focusing on the United States, the estimated acreage-elasticity for maize is 0.30. This estimate falls within the range of micro-level findings reported for the country—generally between 0.01 and 0.95—as summarized in a brief literature review in Gouel and Laborde (2021).

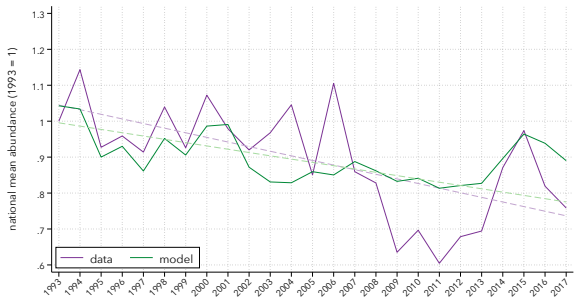
Figure 2: Model fit on national mean abundances of three exemplar species (1993-2017)



(a) Tufted titmouse



(b) Eastern phoebe



(c) Black billed magpie

Notes: Each panel of the above figure plots observed (purple line) and model-predicted (green line) national mean abundances for three exemplar bird species. Dotted lines correspond to linear fits. National mean abundance are normalized by the 1993 historical value. Preliminary results based on OLS estimates of carrying-capacity parameters.

Abundance. The adjusted R^2 from estimating Eq. (49) for all bird species over the 1992-2017 period ranges from 0.59 to 0.97, with a mean of 0.90.[3] To obtain model-based population forecasts, I iterate the growth equation forward in time. Starting from the observed counts in 1992, the OLS-estimated coefficients are applied year-by-year to project the population of each species in each ecoregion up to 2017. Figure 2 plots the time series of observed and model-predicted national mean abundances for three exemplar species. Each species belongs to a different family, occupies a distinct dietary niche, and follows a unique national trend, highlighting the model's ability to capture diverse ecological patterns.

4 Counterfactuals

In this section, I outline the proposed counterfactual exercises and report their results.

[3]In the current version of the paper, carrying-capacity parameters are estimated by OLS. Future versions will explore instrumental-variable strategies to address potential endogeneity in the land-use covariates.

Table 3: Impacts of setting trade costs to their 1980 level on species loss and land-use

		Changes in trade costs		
	Baseline	Inputs + outputs	Inputs	Outputs
	(1)	(2)	(3)	(4)
Regional species loss (av.)	4.33	+9.25%	+5.83%	+2.93%
due to modern ag. (av.)	3.15	+2.15%	-2.25%	+4.31%
due to trad. ag. (av.)	1.17	+22.48%	+19.99%	+1.91%
Share of ag. land (tot.)	0.07	+10.43%	+7.33%	+2.48%
Share of ag. land in modern (tot.)	0.72	-3.79%	-5.23%	+1.56%

Notes: The table reports the baseline value and the percentage changes of listed variables in the counterfactual with trade costs of agricultural inputs and/or agricultural outputs in 1980 relative to the baseline equilibrium of 2011. Preliminary results without considering the livestock sector and grass production in the estimation of the baseline and counterfactual equilibria.

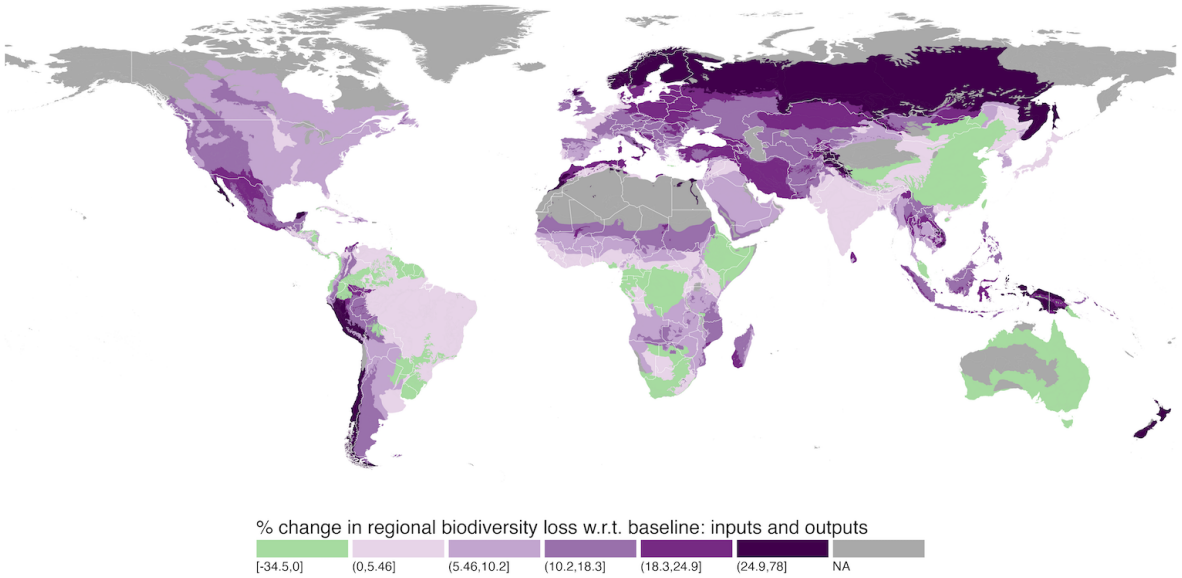
4.1 Methodology

I evaluate how agricultural trade policies affect biodiversity by implementing a set of counterfactual simulations, following the approach of Farrokhi and Pellegrina (2023): all model parameters are held at their 2011 values, while the trade costs for both agricultural inputs and outputs are reset to the 1980 levels. This generates alternative land-use patterns, which are then fed into the ecological sub-models. The resulting species-richness and abundance outcomes are compared with the baseline 2011 scenario, allowing me to isolate the net impact of reduced trade barriers on biodiversity. To disentangle the separate contributions, I run two additional scenarios. In the first, only the input trade costs are set to their 1980 levels while output costs remain at 2011 values, isolating the effect of input liberalization. In the second, only the output trade costs are set to 1980 levels while input costs stay at 2011 levels, revealing the impact of output liberalization alone. By contrasting these three outcomes with the baseline, I can identify how changes in trade costs—both jointly and individually—shape bird biodiversity outcomes. In future work I plan to explore additional counterfactual scenarios, such as a global economy in which all agricultural trade is eliminated.

4.2 Results

Species richness. Table 3 summarizes the average species-richness and global land-use outcomes. Column 1 reflects the baseline economy, where trade costs for both agricultural inputs and outputs are set at their 2011 levels. In that scenario the average number of bird species commited to extinction amounts to 4.33 species per ecoregion. Of these losses, 3.15 species

Figure 3: Spatial distribution of changes in regional species loss with respect to baseline



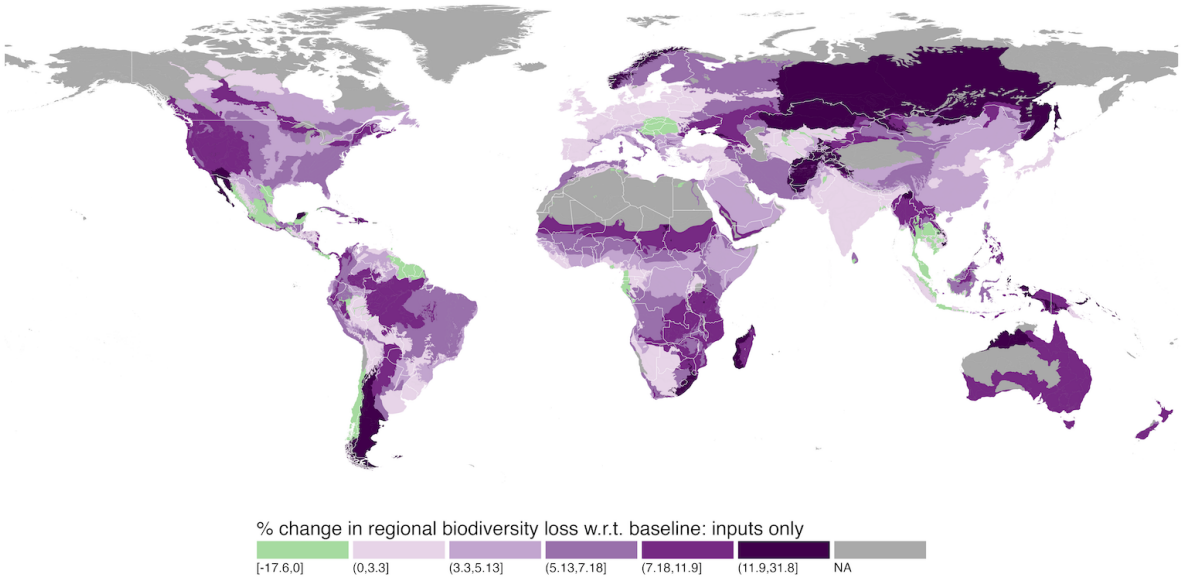
Notes: The figure plots the percentage changes in regional species loss in the counterfactual with trade costs of agricultural inputs and outputs in 1980 relative to the baseline equilibrium of 2011, for each ecoregion. A negative value (in green) indicates that bird species richness is higher in the counterfactual scenario than in the baseline. Preliminary results without considering the livestock sector and grass production in the estimation of the baseline and counterfactual equilibria.

are linked to modern, input-intensive agriculture, while 1.17 species stem from traditional, low-intensity farming. Although agricultural land covers only a small share of the total global land surface (0.07% in the baseline), about 72% of agricultural land is classified as modern. The rest of the table shows that reverting trade costs to their 1980 levels would worsen avian species losses. Under the full-deliberalization scenario (inputs and outputs) the average regional species loss rises by 9.25% relative to the 2011 baseline. The extra loss is driven largely by a significant increase of land-use at the extensive margin exceeding 10%. Although the proportion of modern agricultural land falls slightly (-3.79% overall), the extensive-margin expansion more than offsets any benefit from reduced exposure to agrochemicals, leading to a net increase in habitat conversion and higher extinction risk. Losses attributable to traditional agriculture surge by 22.5% in this counterfactual, while the impact of modern agriculture changes only modestly although higher in the baseline. These findings imply that trade liberalization, such as the one which occured between 1980 and 2011, has the potential to limit bird-species loss, primarily by curbing the spread of extensive, low-intensity farming. It is worth noting, however, that the gains from trade liberalization are partly offset by the intensification of modern agriculture.

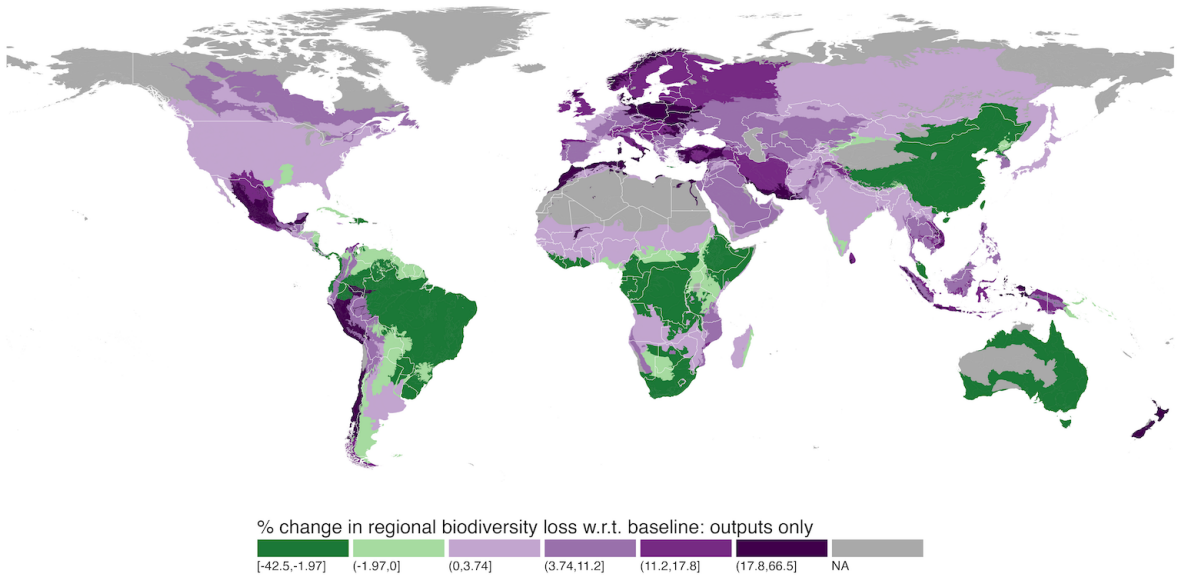
Columns 3 and 4 isolate the effects of altering trade costs for agricultural inputs and outputs respectively. When only the input side becomes more costly (Column 3), the total share of land allocated to agriculture expands by over 7%. At the same time, the proportion

Figure 4: Decomposition of the impact of setting trade costs to their 1980 level on regional species loss by good type

(a) Only agricultural inputs



(b) Only agricultural outputs



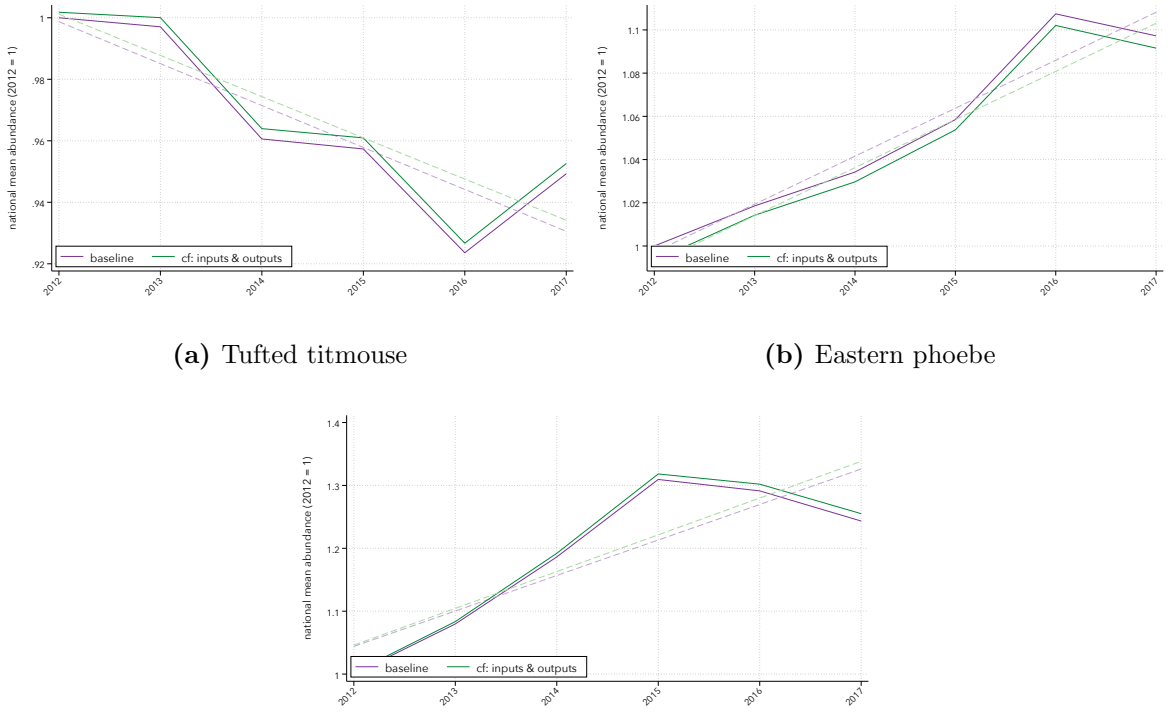
Notes: The figure plots the percentage changes in regional species loss in the counterfactual with trade costs of agricultural inputs (panel a) or agricultural outputs (panel b) in 1980 relative to the baseline equilibrium of 2011, for each ecoregion. A negative value (in green) indicates that bird species richness is higher in the counterfactual scenario than in the baseline. Preliminary results without considering the livestock sector and grass production in the estimation of the baseline and counterfactual equilibria.

of that land classified as modern falls by about 5%, indicating a shift toward more traditional farming practices. This reallocation has two contrasting consequences on biodiversity. The modest decline in the species-loss component associated with modern agriculture indicates that the retreat of intensive farming marginally alleviates pressure on ecosystems. In stark contrast, the species-loss component associated with traditional agriculture rises by more than 22%, driven by small-holder farms expanding cultivation into previously undisturbed habitats. When these opposing effects are aggregated, the net outcome is a deterioration in biodiversity: the overall number of species projected to face extinction rises by close to 6%. Hence, the escalation of input trade costs principally drives land-use expansion, overwhelming the modest biodiversity gains derived from a reduced footprint of modern agriculture. Increasing trade costs on the output side (Column 4) generates a qualitatively different response. Higher export barriers diminish the profitability of specialization, compelling nations to produce more for domestic consumption, including crops for which they lack comparative advantage. Because the agro-ecological conditions for these crops are sub-optimal, producers must apply greater quantities of inputs to attain acceptable yields. Pressures at both the extensive and intensive margins produce an increase in average regional species loss of roughly 3%. However, the output-cost channel appears less of a driver of biodiversity change than the input-cost channel.

Figure 3 shows the spatial distribution of biodiversity gains and losses in the counterfactual economy. It confirms that raising trade costs for both outputs and inputs generally leads to greater biodiversity loss across most ecoregions. However, the average outcomes reported earlier mask substantial spatial heterogeneity. In several ecoregions, the number of bird species driven toward extinction rises by as much as 78% when trade costs revert to their 1980 levels, underscoring the sizable benefit of trade liberalization in averting losses. Conversely, many southern ecoregions experience improved biodiversity under deliberalization, with the number of threatened species falling by up to 34.5%. As illustrated in Appendix Figure A.2, the regions that suffer under liberalization are precisely those with the highest pre-anthropocene species richness. These findings suggest that agricultural trade liberalization policies can curb global biodiversity loss overall, but at the cost of key southern biodiversity hotspots. Disentangling the effects of input-cost and output-cost adjustments clarifies the mechanisms at work. As shown in Figure 4, liberalizing outputs while keeping trade in inputs costly increases biodiversity loss in the affected regions relative to the baseline. The reverse pattern emerges when inputs are liberalized but output trade costs remain high: biodiversity improves in these hotspots. Consequently, liberalizing agricultural output markets tends to push production southward into biodiversity-rich areas. Although reductions in inputs trade costs can partially offset habitat conversion by boosting productivity, the first effect dominates, leading to net biodiversity loss.

Abundance. Figure 5 displays the medium-run dynamics of three bird species under two conditions: the baseline and a counterfactual scenario in which both output and input trade

Figure 5: Impacts of setting trade costs to their 1980 level on the population dynamics of three exemplar species (2012-2017)



(a) Tufted titmouse

(b) Eastern phoebe

(c) Black billed magpie

Notes: Each panel of the above figure plots baseline (purple line) and counterfactual (green line) national mean abundances for three exemplar bird species. In the counterfactual scenario, both input and output trade costs are set to their 1980 level. Dotted lines correspond to linear fits. National mean abundance are normalized by the 2012 historical value. Preliminary results based on OLS estimates of carrying-capacity parameters and without considering the livestock sector and grass production in the estimation of the baseline and counterfactual equilibria.

costs are set to their 1980 levels.[4] Land use is shocked once—in 2011—and the population-dynamics model projects abundances for the ensuing years. The results confirm that trade policies shape the population trajectories of common U.S. birds, with effects that are heterogeneous across species. Among the three exemplar species, the national-mean abundance of the tufted titmouse and the black-billed magpie would be slightly higher under the counterfactual—by 0.3 and 1.2 percentage points (p.p.) at the end of the period, respectively—while the eastern phoebe's abundance would be 0.6 p.p. lower. Crucially, the gap between baseline and counterfactual widens over time for the black-billed magpie, consistent with the compounding nature of population dynamics and suggesting that the full ecological footprint of current trade policy may only become apparent over longer horizons. Two caveats are worth

[4]The carrying-capacity parameters used in the population-dynamics module are estimated by OLS. Future versions of the paper will explore instrumental-variable strategies to address potential endogeneity in the land-use covariates.

noting. First, the model aggregates pesticide use by total quantity, ignoring differences among active ingredients; if recent agro-chemical innovations have introduced more toxic compounds at lower application rates, the model may underestimate intensive-margin biodiversity loss. Second, the model does not yet account for changes in land use and climate within ecoregions where these species overwinter, a limitation that forthcoming versions of the paper will address.

Feedback effects on agriculture, trade and welfare. To be completed.

5 Conclusion

This paper asks whether agricultural trade liberalization erodes biodiversity or helps preserve it—a question with profound consequences for how we design trade agreements and conservation policy. To answer it, I develop the first quantitative trade model in which biodiversity is an endogenous outcome, linking a multi-country Ricardian trade framework to ecological models. The framework allows trade-cost changes to propagate through land-use decisions at both the extensive and intensive margins, and ultimately into ecological outcomes measured by species richness and population abundance.

The results cut against the presumption that freer trade is detrimental to biodiversity: the liberalization that took place between 1980 and 2011 has, on average, reduced the number of bird species committed to extinction. By raising agricultural productivity and enabling specialization according to comparative advantage, lower trade costs reduced the total land area needed for food production, curbing the spread of extensive low-intensity farming. Reverting to 1980 trade costs would raise average species loss per ecoregion by 9.25%, driven by a 10% expansion of the agricultural frontier. This aggregate result, however, conceals a stark spatial asymmetry. Southern biodiversity hotspots bear the cost of liberalization, as lower output trade costs shift production toward regions where agro-ecological conditions confer comparative advantage in many crops. Northern ecoregions, by contrast, are spared further conversion. Trade-induced land-use changes also leave a modest but persistent imprint on U.S. bird population dynamics, with simulated national-average abundances shifting by 0.3–1.2 percentage points over five years following the trade-cost shock. The direction and magnitude of these effects vary across species, reflecting their differing sensitivities to habitat loss and pesticide exposure.

These findings carry direct policy implications. They suggest that trade liberalization is not simply an accelerant of biodiversity loss. Its aggregate effect can be protective, primarily by reducing pressure at the extensive margin. At the same time, the concentration of losses in southern biodiversity hotspots implies that the ecological costs of liberalization are borne disproportionately by the regions most irreplaceable from a conservation standpoint. This points to a need for trade agreements to be accompanied by targeted conservation policies in

biodiversity-rich regions, and for biodiversity impacts to be incorporated into the standard welfare calculus of trade policy evaluation.

The paper has several limitations that future work will address. First, the current quantitative exercise omits the livestock sector and grass production, which may bias estimates of biodiversity effects given that pasture accounts for the majority of global agricultural land. Second, the abundance module does not account for migratory connectivity: many bird species split their annual cycle between distant breeding and wintering grounds, so that conservation efforts in one region may be undermined if ecological pressures persist where those species spend the rest of the year. Accounting for these cross-border ecological linkages would reveal the extent to which biodiversity outcomes depend on coordination across countries, offering new insights for the design of multilateral environmental policies. Finally, the feedback from trade-induced biodiversity change to agricultural productivity, land-use decisions, and welfare remains to be fully quantified. If trade liberalization erodes biodiversity in certain regions, and biodiversity loss in turn reduces crop yields—through diminished pest control and pollination—then the conventional gains from trade are overstated.

References

Allen, T. and C. Arkolakis. 2014. "Trade and the Topography of the Spatial Economy." *The Quarterly Journal of Economics* 129 (3):1085–1140.

Anderson, Kym, Marianne Kurzweil, Will Martin, Damiano Sandri, and Ernesto Valenzuela. 2008. "Measuring Distortions to Agricultural Incentives, Revisited." *World Trade Review* 7 (3):675–704.

Arellano, Manuel and Stephen Bond. 1991. "Some Tests of Specification for Panel Data: Monte Carlo Evidence and an Application to Employment Equations." *The Review of Economic Studies* 58 (2):277–297.

Cabernard, L., S. Pfister, and S. Hellweg. 2024. "Biodiversity Impacts of Recent Land-Use Change Driven by Increases in Agri-Food Imports." *Nature Sustainability* 7 (11):1512–1524.

Carleton, T., L. Crews, and I. Nath. 2025. "Agriculture, Trade, and the Spatial Efficiency of Global Water Use." .

Chaudhary, A. and T. M. Brooks. 2018. "Land Use Intensity-Specific Global Characterization Factors to Assess Product Biodiversity Footprints." *Environmental Science & Technology* 52 (9):5094–5104.

Chaudhary, A. and T. Kastner. 2016. "Land Use Biodiversity Impacts Embodied in International Food Trade." *Global Environmental Change* 38:195–204.

Chaudhary, A., F. Verones, L. de Baan, and S. Hellweg. 2015. "Quantifying Land Use Impacts on Biodiversity: Combining Species–Area Models and Vulnerability Indicators." *Environmental Science & Technology* 49 (16):9987–9995.

Cocco, V., Y. Kervinio, and L. Mouysset. 2023. "Relaxing the Production-Conservation Trade-off: Biodiversity Spillover in the Bioeconomic Performance of Ecological Networks." *Ecological Economics* 214:107966.

Comin, D;, D. Lashkari, and M. Mestieri. 2021. "Structural Change With Long-Run Income and Price Effects." *Econometrica* 89 (1):311–374.

Costinot, A., D. Donaldson, and C. Smith. 2014. "Evolving Comparative Advantage and the Impact of Climate Change in Agricultural Markets: Evidence from 1.7 Million Fields around the World." *Journal of Political Economy* 124.

Dominguez-Iino, T. 2025. "Efficiency and Redistribution in Environmental Policy: An Equilibrium Analysis of Agricultural Supply Chains."

Eng, Margaret L., Bridget J. M. Stutchbury, and Christy A. Morrissey. 2019. "A Neonicotinoid Insecticide Reduces Fueling and Delays Migration in Songbirds." *Science* 365 (6458):1177–1180.

Farrokhi, D. and H. S. Pellegrina. 2023. "Trade, Technology, and Agricultural Productivity." *Journal of Political Economy* 131 (9):2509–2555.

Farrokhi, F., E. Kang, H. S. Pellegrina, and S. Sotelo. 2025. "Deforestation: A Global and Dynamic Perspective."

Fischer, G., F.O. Nachtergaele, H.T. van Velthuizen, F. Chiozza, G. Franceschini, M. Henry, D. Muchoney, and S. Tramberend. 2021. *Global Agro-Ecological Zones v4 – Model documentation.* Rome, FAO.

Frank, E. and A. Sudarshan. 2024. "The Social Costs of Keystone Species Collapse: Evidence from the Decline of Vultures in India." *American Economic Review* 114 (10):3007–40.

Gouel, C. and D. Laborde. 2021. "The Crucial Role of Domestic and International Market-Mediated Adaptation to Climate Change." *Journal of Environmental Economics and Management* 106:102408.

Hummels, David. 2007. "Transportation Costs and International Trade in the Second Era of Globalization." *Journal of Economic Perspectives* 21 (3):131–154.

Lopez-Antia, Ana, Manuel E. Ortiz-Santaliestra, François Mougeot, and Rafael Mateo. 2015. "Imidacloprid-Treated Seed Ingestion Has Lethal Effect on Adult Partridges and Reduces Both Breeding Investment and Offspring Immunity." *Environmental Research* 136:97–107.

Mariyappan, M., M. Rajendran, S. Velu, A. D. Johnson, G. K. Dinesh, K. Solaimuthu, M. Kaliyappan, and M. Sankar. 2023. "Ecological Role and Ecosystem Services of Birds: A Review." *International Journal of Environment and Climate Change* 13 (6):76–87.

Mouysset, L., C. Rais Assa, J-S. Ay, F. Jiguet, R. Lorrilière, and L. Doyen. 2019. "Bioeconomic Impacts of Agroforestry Policies in France." *Land Use Policy* 85:239–248.

Nickell, Stephen. 1981. "Biases in Dynamic Models with Fixed Effects." *Econometrica* 49 (6):1417–1426.

Noack, F., D. Engist, and A. Larsen. 2025. "The Value of Biodiversity: Evidence from Migratory Birds."

Olson, D. M., E. Dinerstein, E. D. Wikramanayake, N. D. Burgess, G. V. N. Powell, E. C. Underwood, J. A. D'amico, I. Itoua, H. E. Strand, J. C. Morrison, C. J. Loucks, T. F. Allnutt, T. H. Ricketts, Y. Kura, J. F. Lamoreux, W. W. Wettengel, P. Hedao, and K. R. Kassem. 2001. "Terrestrial Ecoregions of the World: A New Map of Life on Earth." *BioScience* 51 (11):933.

Padoa-Schioppa, E., M. Baietto, R. Massa, and L. Bottoni. 2006. "Bird Communities as Bioindicators: The Focal Species Concept in Agricultural Landscapes." *Ecological Indicators* 6 (1):83–93.

Pardieck, K. L, D. Ziolkowski Jr., M. Lutmerding, V. Aponte, and M.-A. R. Hudson. 2020. "North American Breeding Bird Survey Dataset 1966 - 2019, Version 2019.0."

Pereira, H. M. and G. C. Daily. 2006. "Modeling Biodiversity Dynamics in Countryside Landscapes." 87 (8):1877–1885.

Polasky, Stephen, Christopher Costello, and Carol McAusland. 2004. "On Trade, Land-Use, and Biodiversity." *Journal of Environmental Economics and Management* 48 (2):911–925.

Ramankutty, N., A. T. Evan, C. Monfreda, and J. A. Foley. 2008. "Farming the planet: 1. Geographic distribution of global agricultural lands in the year 2000." *Global Biogeochemical Cycles* 22 (1).

Rigal, S., V. Dakos, H. Alonso, A. Auniņš, Z. Benkő, L. Brotons, T. Chodkiewicz, P. Chylarecki, E. de Carli, J. C. del Moral, C. Domşa, V. Escandell, B. Fontaine, R. Foppen, R. Gregory, S. Harris, S. Herrando, M. Husby, C. Ieronymidou, F. Jiguet, J. Kennedy, A. Klvaňová, P. Kmecl, L. Kuczyński, P. Kurlavičius, J. A. Kålås, A. Lehikoinen, A. Lindström, R. Lorrillière, C. Moshøj, R. Nellis, D. Noble, D. P. Eskildsen, J.-Y. Paquet, M. Pélissié, C. Pladevall, D. Portolou, J. Reif, H. Schmid, B. Seaman, Z. D. Szabo, T. Szép, G. T. Florenzano, N. Teufelbauer, S. Trautmann, C. van Turnhout, Z. Vermouzek, T. Vikstrøm, P. Voříšek, A. Weiserbs, and V. Devictor. 2023. "Farmland Practices Are Driving Bird Population Decline across Europe." *Proceedings of the National Academy of Sciences* 120 (21):e2216573120.

Scherer, L., F. Rosa, Z. Sun, O. Michelsen, V. De Laurentiis, A. Marques, S. Pfister, F. Verones, and K. J. J. Kuipers. 2023. "Biodiversity Impact Assessment Considering Land Use Intensities and Fragmentation." *Environmental Science & Technology* 57 (48):19612–19623.

WWF. 2024. "Living Planet Report 2024: A System in Peril." Tech. rep., WWF International, Gland, Switzerland.

A Appendix

A.1 Additional figures

Figure A.1: Distribution of NABBS routes and cropland across the United States

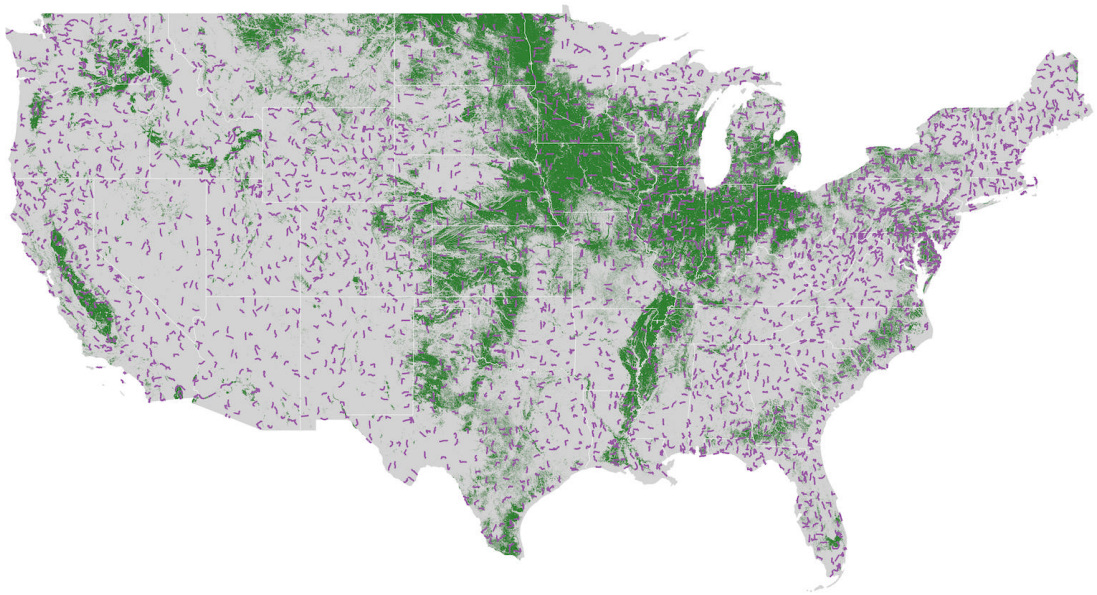


Figure A.2: Pre-anthropocene regional species richness

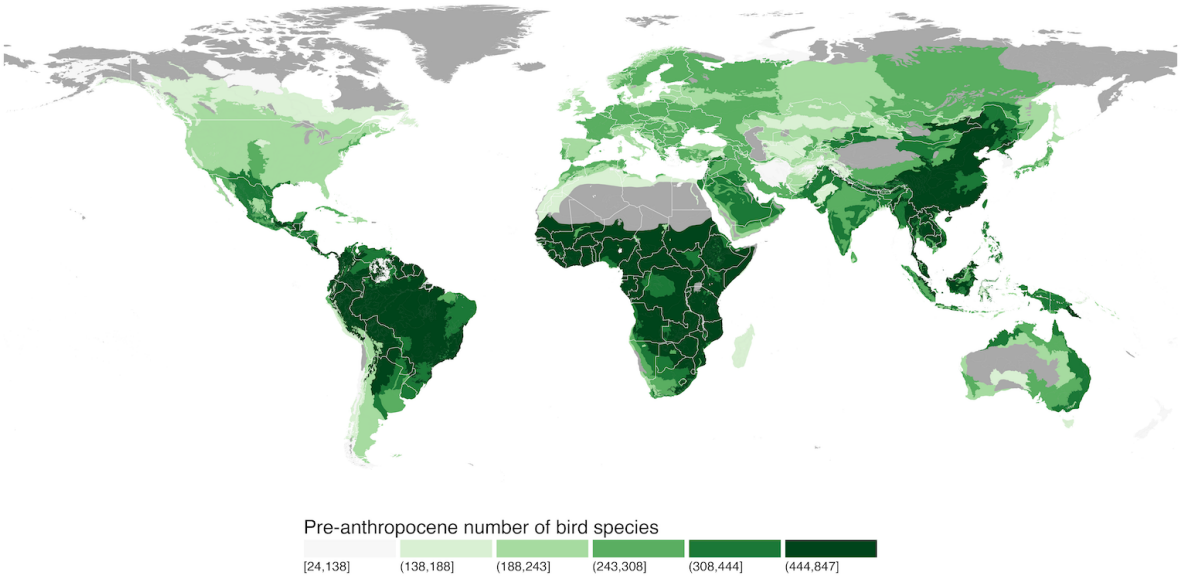
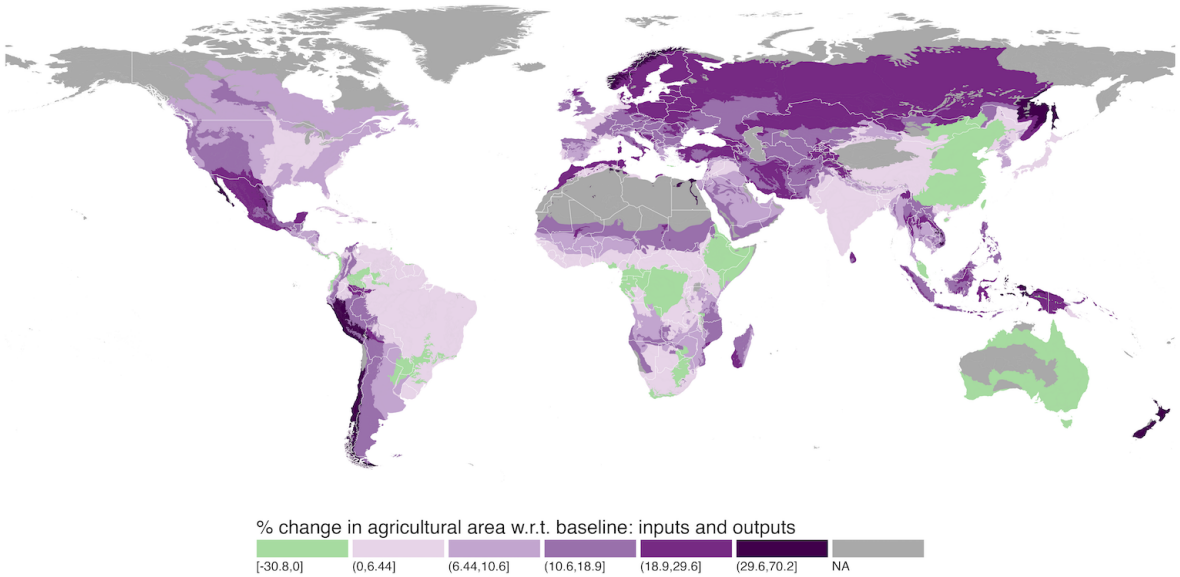
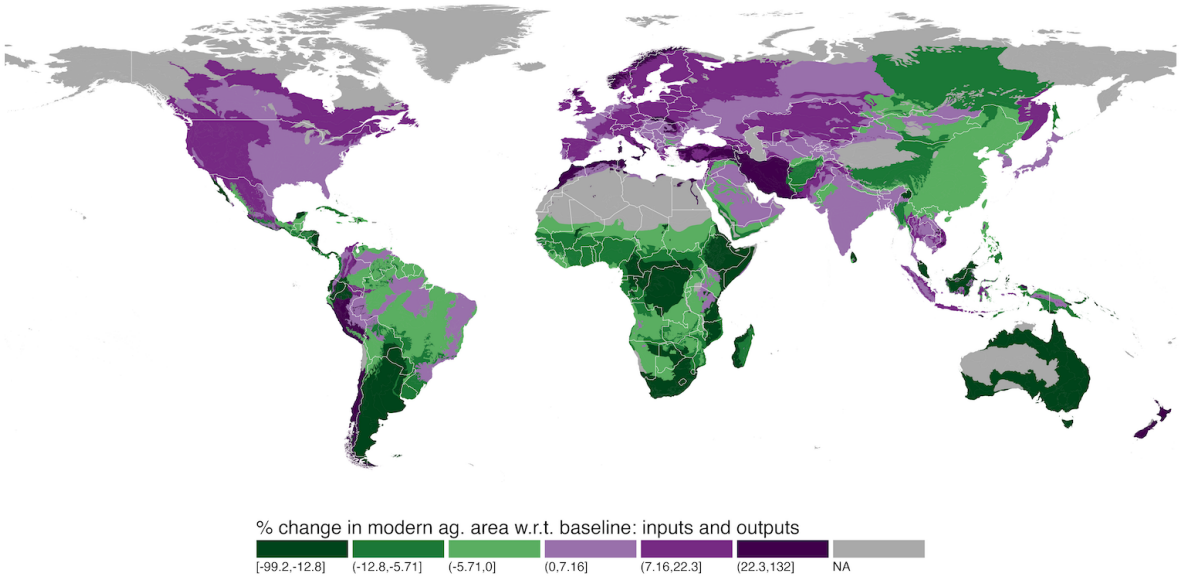


Figure A.3: Impact of setting input and output trade costs to their 1980 level on land-use

(a) Agricultural area



(b) Modern area within agriculture



Notes: Preliminary results without livestock sector and grass production.